

Jets, tidal disruption and lenses

Plan and reviews

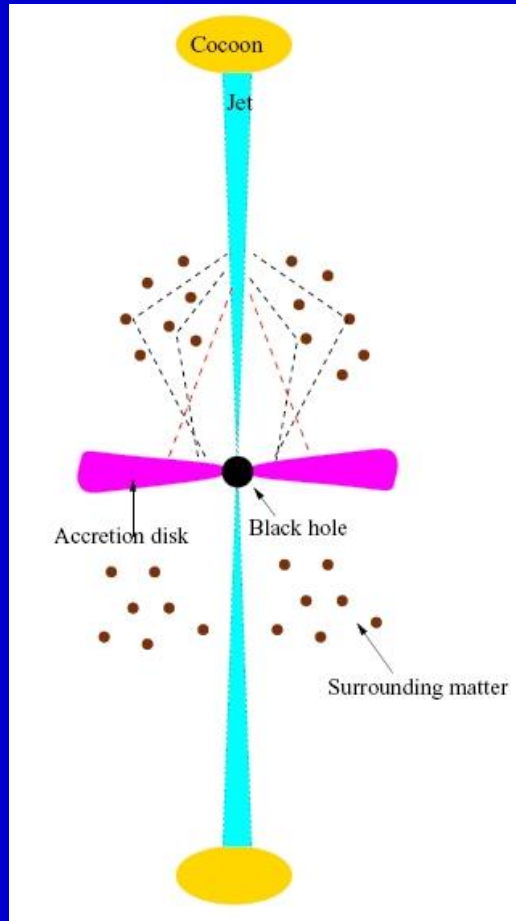
Plan

1. Jets: AGNs and close binary systems
2. Tidal disruption of stars by SMBHs
3. Spectral lines and lensing

Reviews

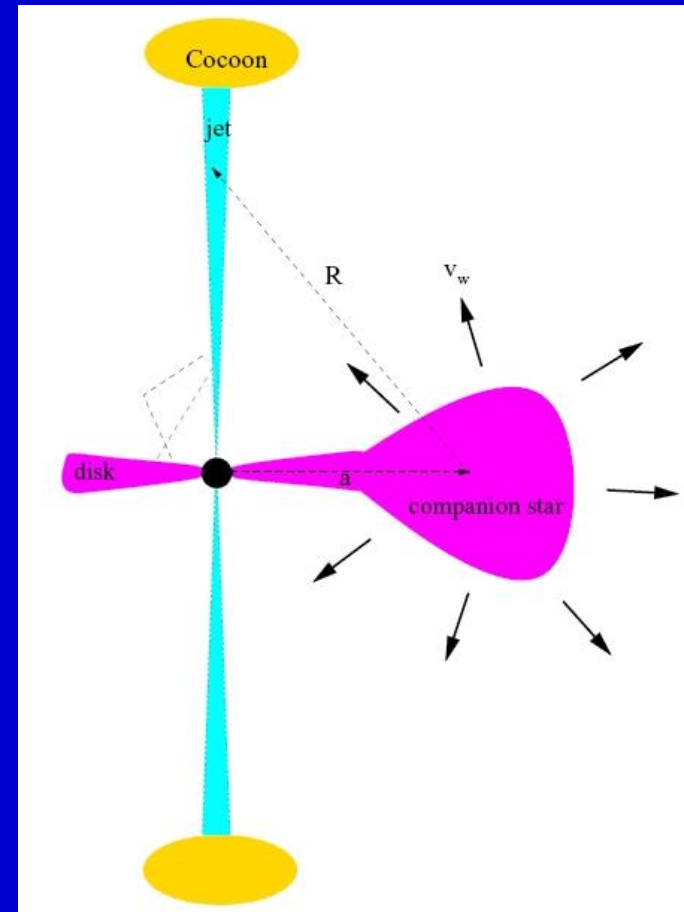
- [astro-ph/0611521](#) **High-Energy Aspects of Astrophysical Jets**
- [astro-ph/0306429](#) **Extreme blazars**
- [astro-ph/0312545](#) **AGN Unification: An Update**
- [astro-ph/0212065](#) **Fluorescent iron lines as a probe of astrophysical black hole systems**
- [arXiv: 1104.0006](#) **AGN jets**
- [astro-ph/0406319](#) **Astrophysical Jets and Outflows**
- [arXiv: 1309.4772](#) **Blazars: jets and discs**
- [arXiv: 1707.07134](#) **AGNs of different types**

Jets in AGNs and close binaries



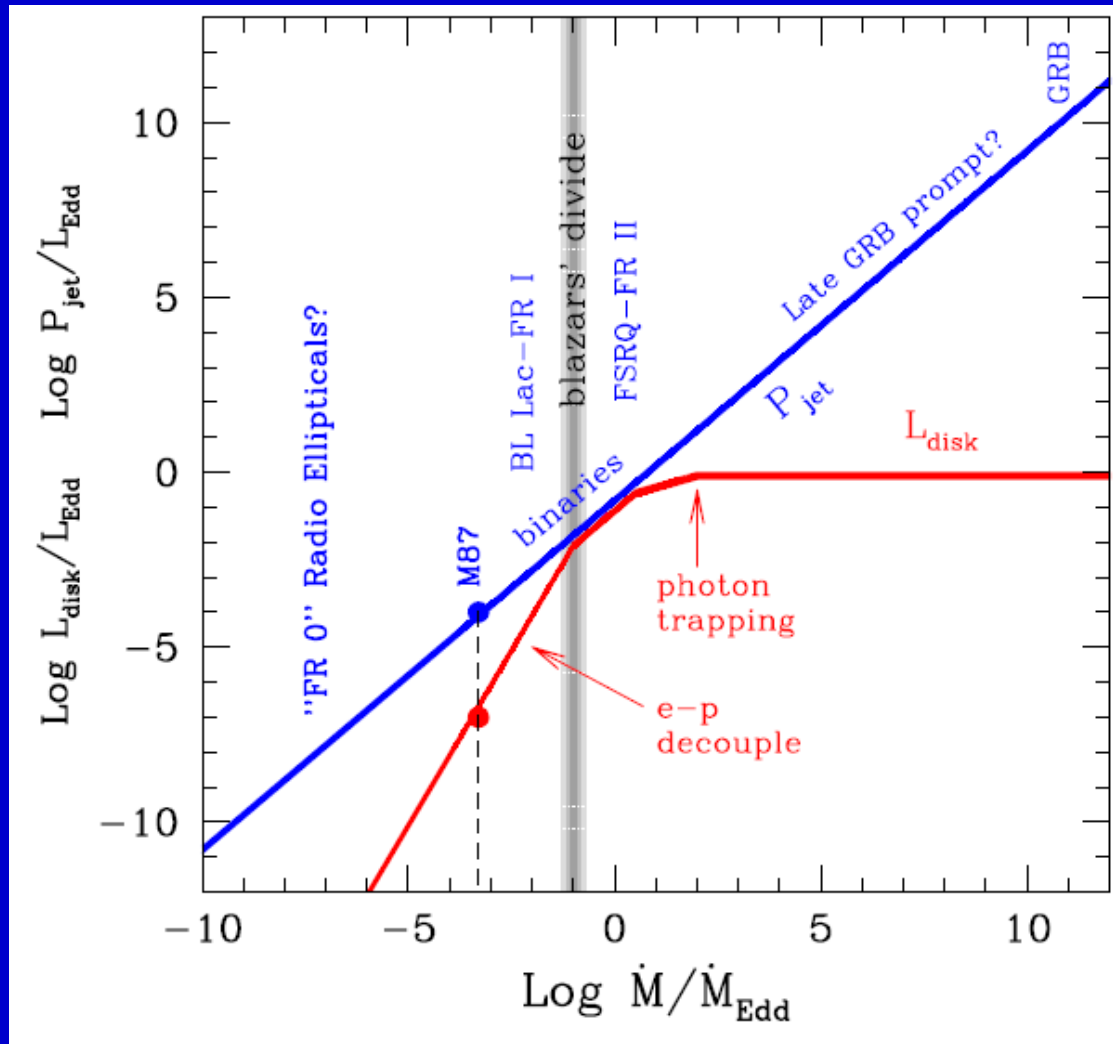
AGN: $M_{\text{BH}} = 10^8 - 10^9 M_{\odot}$
 $L < \sim L_{\text{Edd}} \sim 10^{42} - 10^{47} \text{ erg/s}$
< few Mpc
 $\Gamma \sim 5 - 50$
 $\Delta t \sim \text{hours-years}$

CBS: $M_{\text{BH}} \sim 10 M_{\odot}$
 $L < \sim L_{\text{Edd}} \sim 10^{37} - 10^{40} \text{ erg/s}$
 $\sim \text{pc}$
 $\Gamma \sim 1 - 10$
 $\Delta t \sim \text{days}$



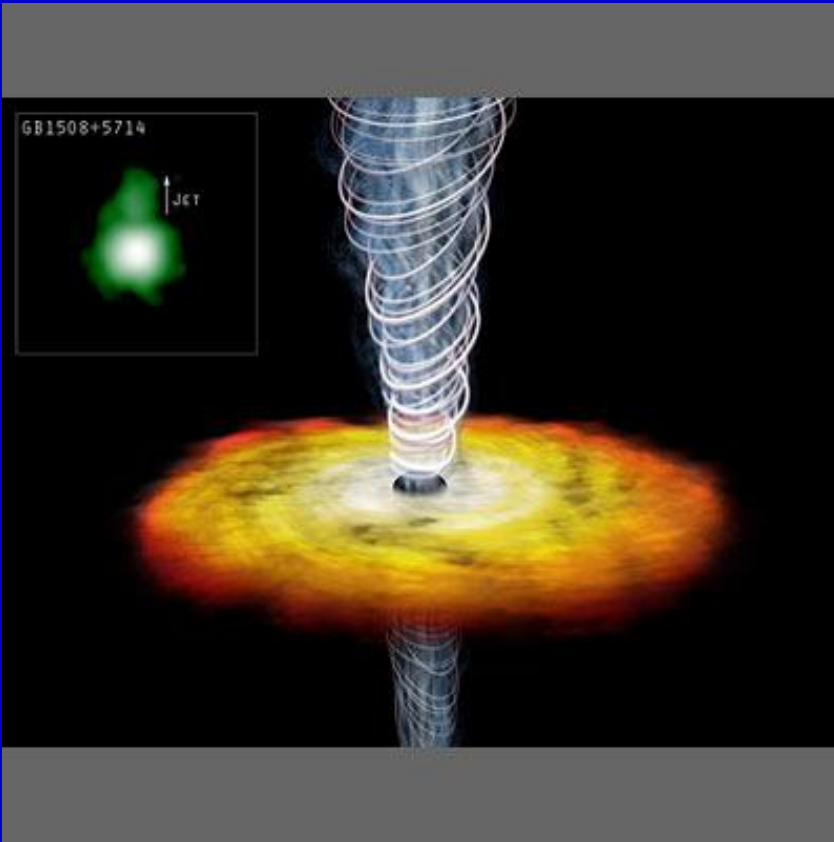
see astro-ph/0611521

All jets in one plot

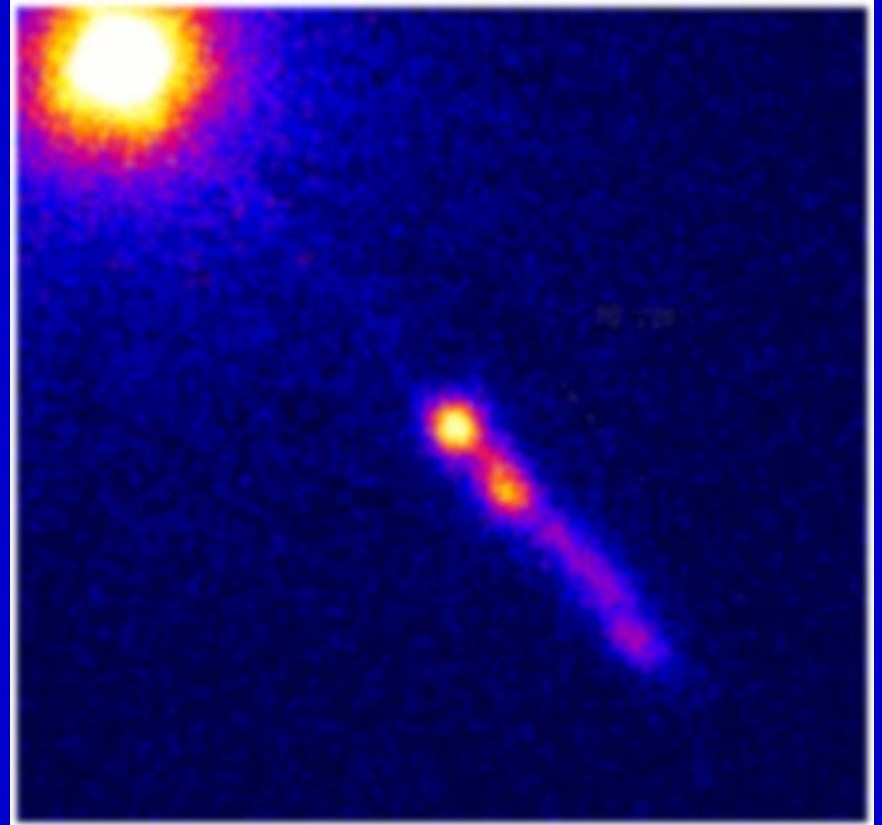


Close-by and far-away jets

1% of SMBH are active. 10% out of them launch relativistic jets.
Jets are not magnetically dominated.



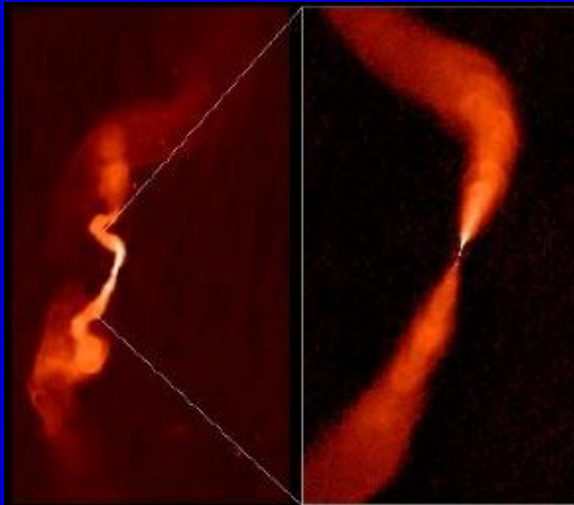
GB1508+5714 $z=4.30$



3C273

See a review in 1104.0006

Classification of AGN radio jets



FR Class I source: radio galaxy 3C31

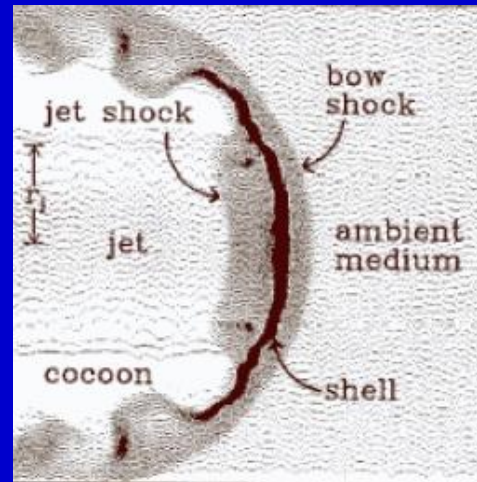


FR Class II source: quasar 3C175

FR I. Two-sided jets.

Jets dominate in the emission.

Usually are found in rich clusters.



FR II. One-sided jets.

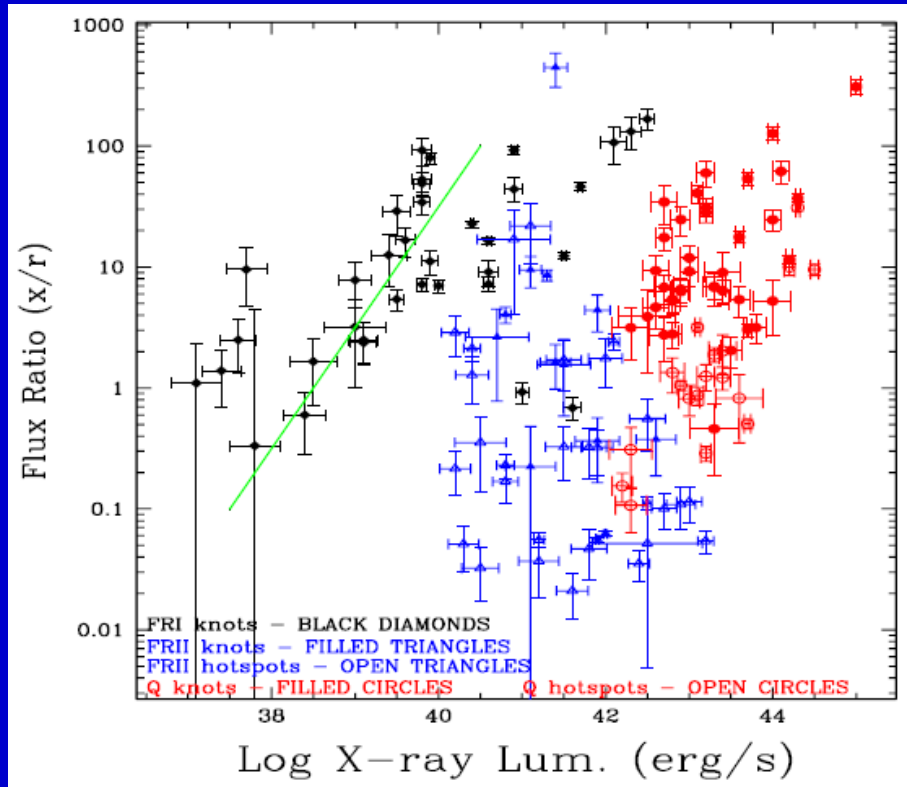
Radio lobes dominate over jets.

Mostly isolated galaxies
or poor groups.

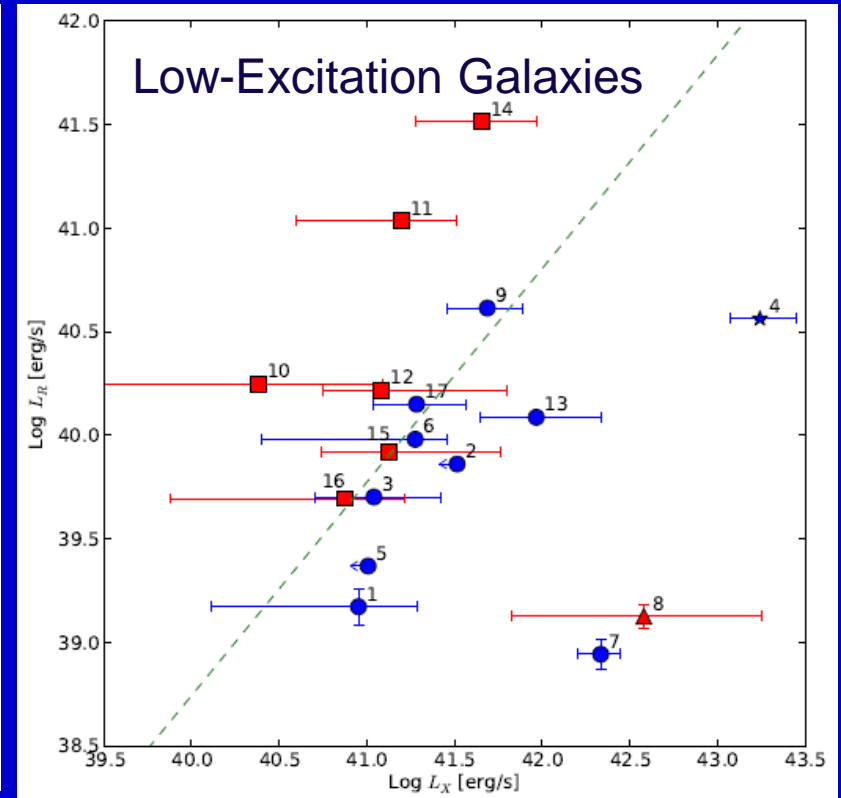
astro-ph/0406319

See a review on radio galaxies in arXiv: 1101.0837

X-ray and radio properties



1003.0976



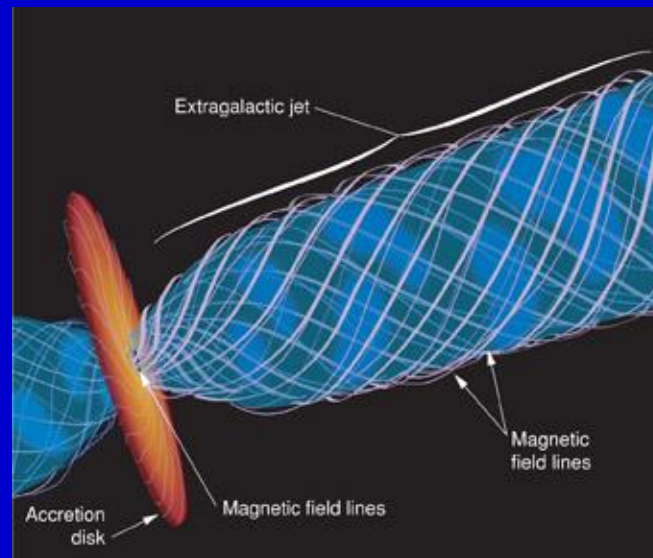
1104.3575

Magnetic field in a jet



Observations of M87 tell us that the magnetic field in the jet is mostly parallel to the jet axis, but in the emission regions (“knots”) it becomes perpendicular (see [astro-ph/0406319](https://arxiv.org/abs/astro-ph/0406319)).

The same structure is observed in several jets with radio lobes.

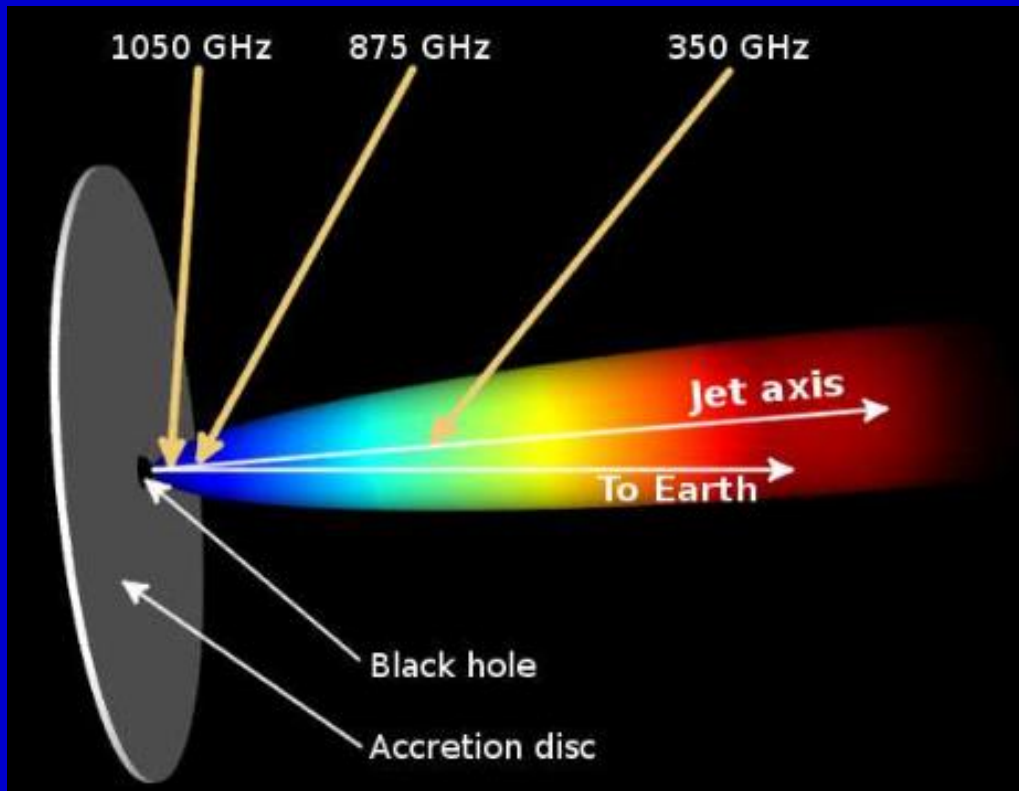


New RadioAstron data give some new insights.

Magnetic field in the jet

Due to modern high resolution observations new important results on the magnetic field in jets are obtained.

ALMA 0.01 pc scale

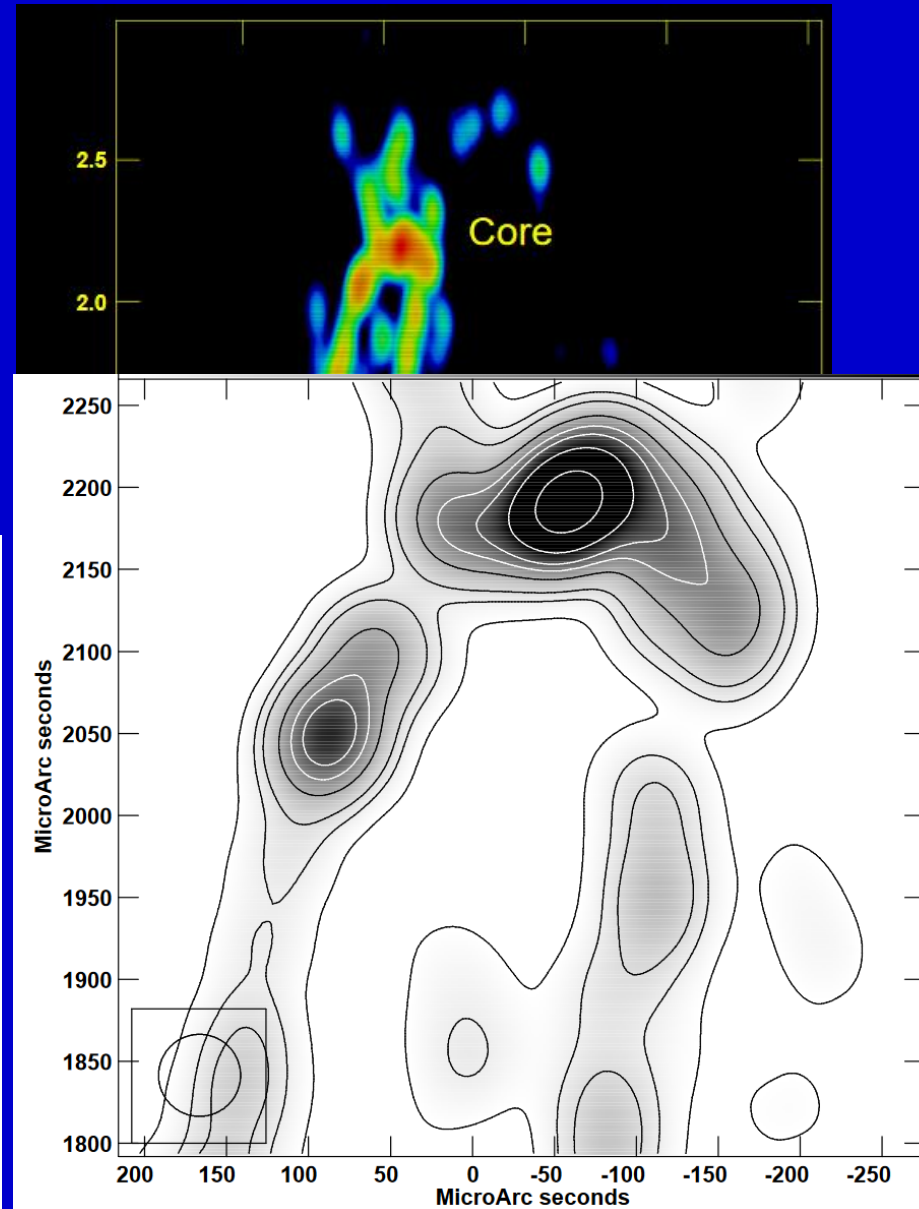
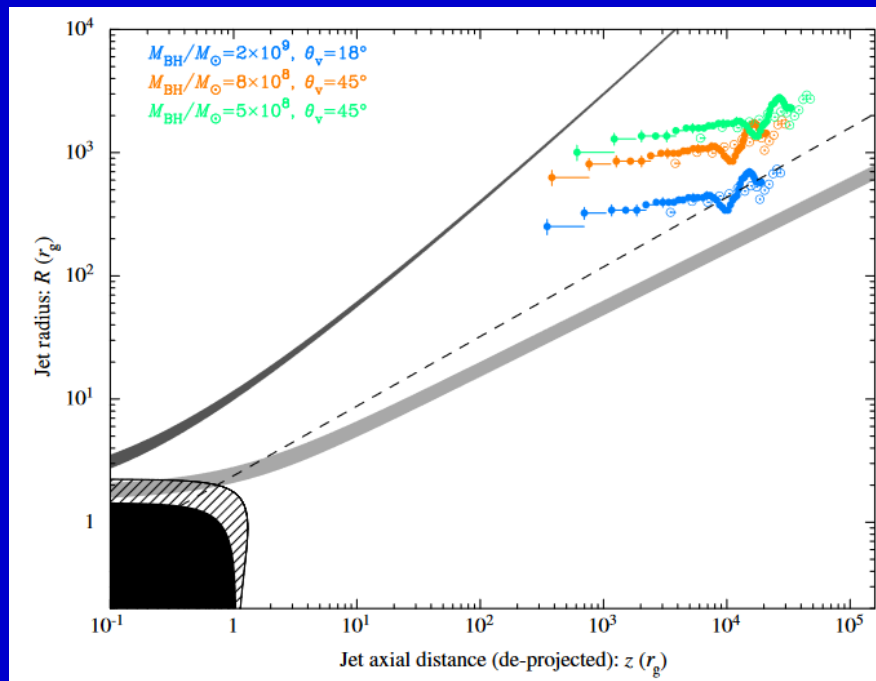


Magnetic fields of at least tens of Gauss (and possibly considerably higher) on scales of the order of light days (0.01 pc) from the black hole.

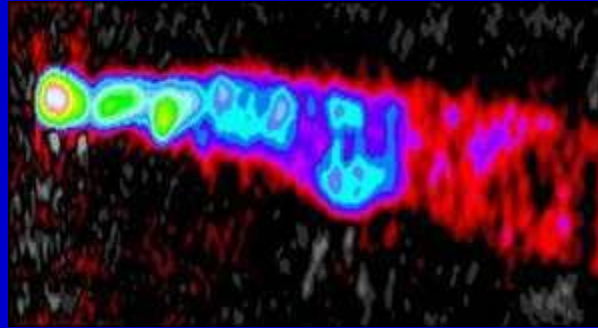
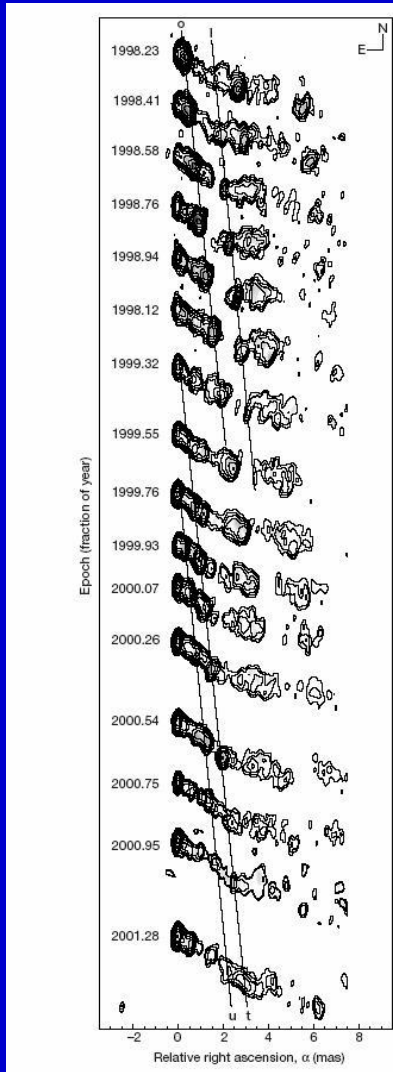
3C84 jet

Jet followed down to $>\sim 100 R_{\text{sh}}$
BH mass $\sim 2 \cdot 10^9$

Jet from the disc, not from ergosphere?



Blobs in jets

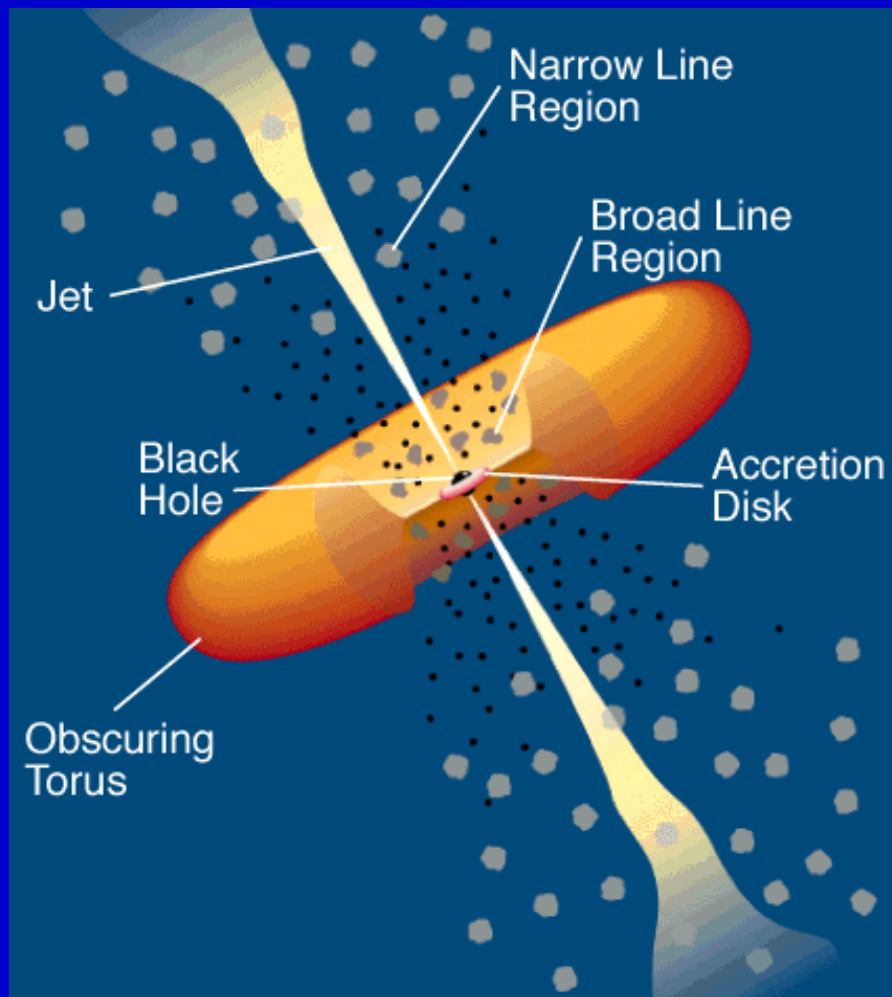


It is believed that bright features in AGN jets can be results of the Kelvin-Helmholtz instability. This instability leads to a spiral structure formation in a jet. (see, for example, astro-ph/0103379).

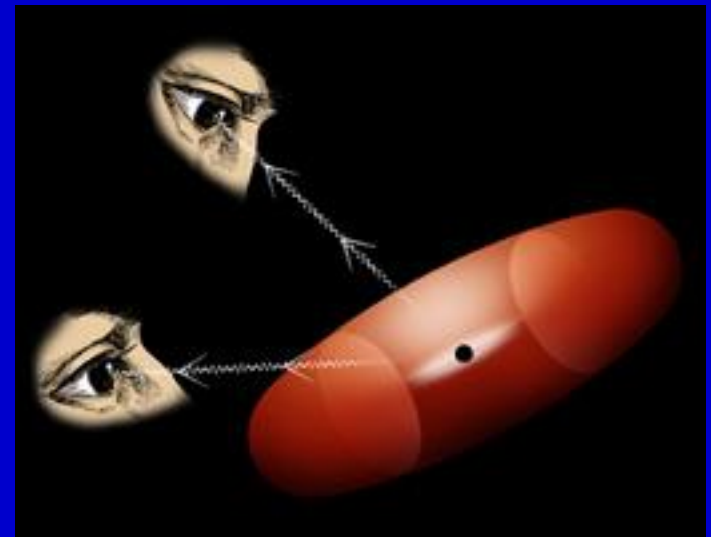
3C 120

However, in the case of 3C 120 the blobs appearance is due to processes in the disc. Dips in X-rays (related to the disc) appear before blobs ejection (Marscher et al. 2002).

Blazars



If a jet is pointing towards us, then we see a *blazar*.



Blazars at very high energies

Blazars are powerful gamma-ray sources. The most powerful of them have equivalent isotropic luminosity 10^{49} erg/s.

Collimation $\theta^2/2 \sim 10^{-2} - 10^{-3}$. θ – jet opening angle.

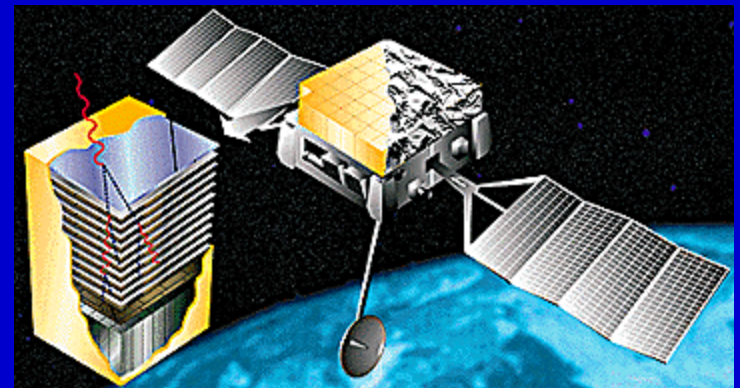
EGRET detected 66 (+27) sources of this type.

New breakthrough is expected after the launch of GLAST.

Several sources have been detected in the TeV range by ground-based gamma-ray telescopes. All of them, except M87, are BL Lacs at $z < 0.2$ (more precisely, to high-frequency-peaked BL Lac – HBL).

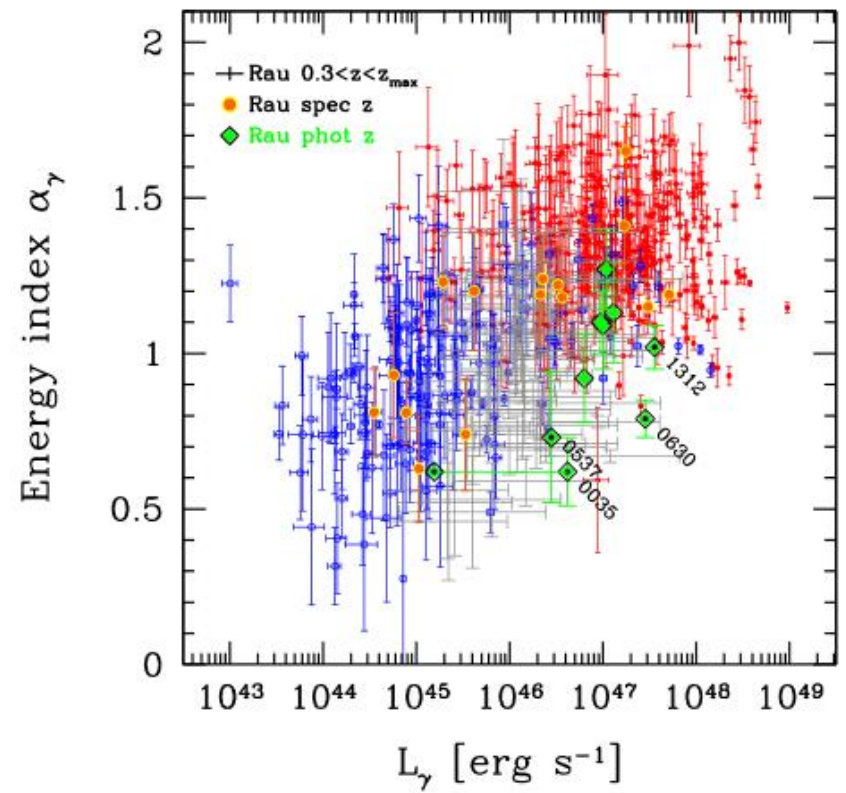
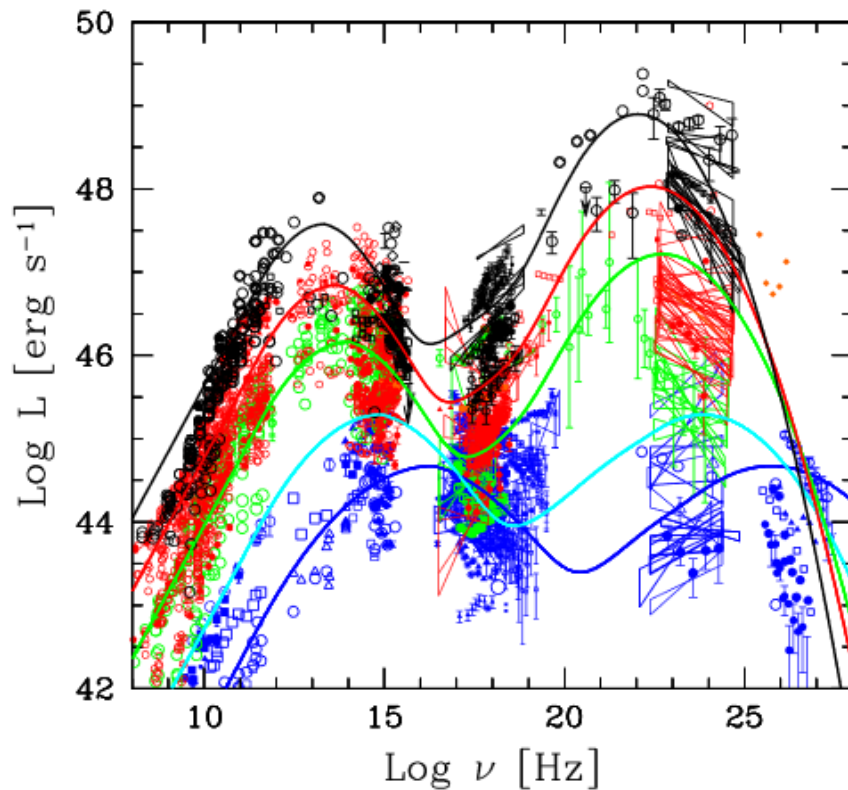
Observations show that often (but not always) after a gamma-ray bursts few weeks or months later a burst happens also in the radio band.

(see astro-ph/0611521)

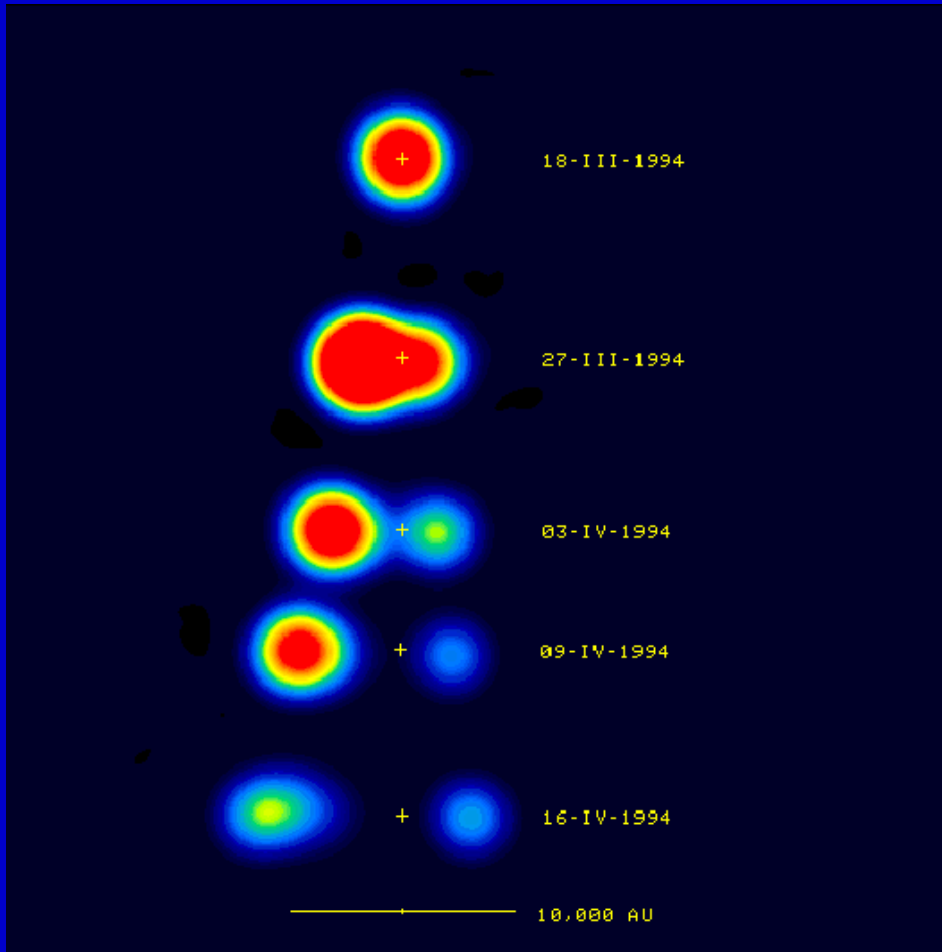


Fermi

Blazar spectra



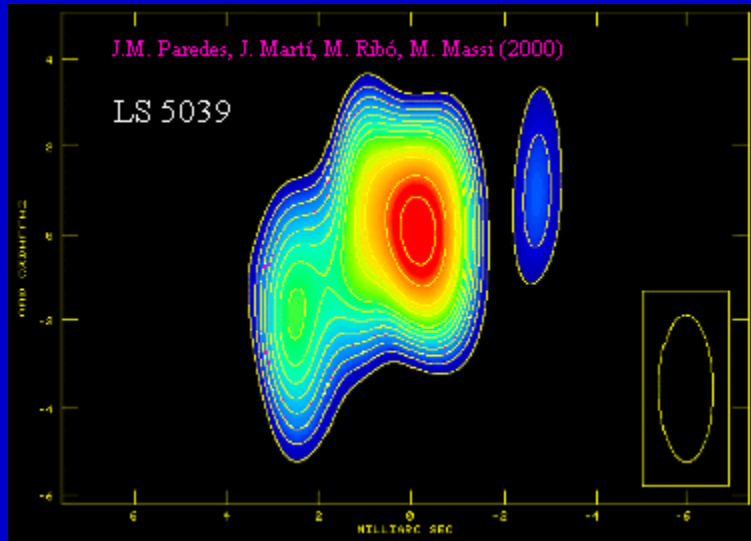
Microquasars



GRS 1915

The correlation between X-ray and synchrotron (i.e. between disc and jet emission) is observed.

Microquasars jets in radio



LS 5039/RX J1826.2-1450 –
is a galactic massive X-ray binary.

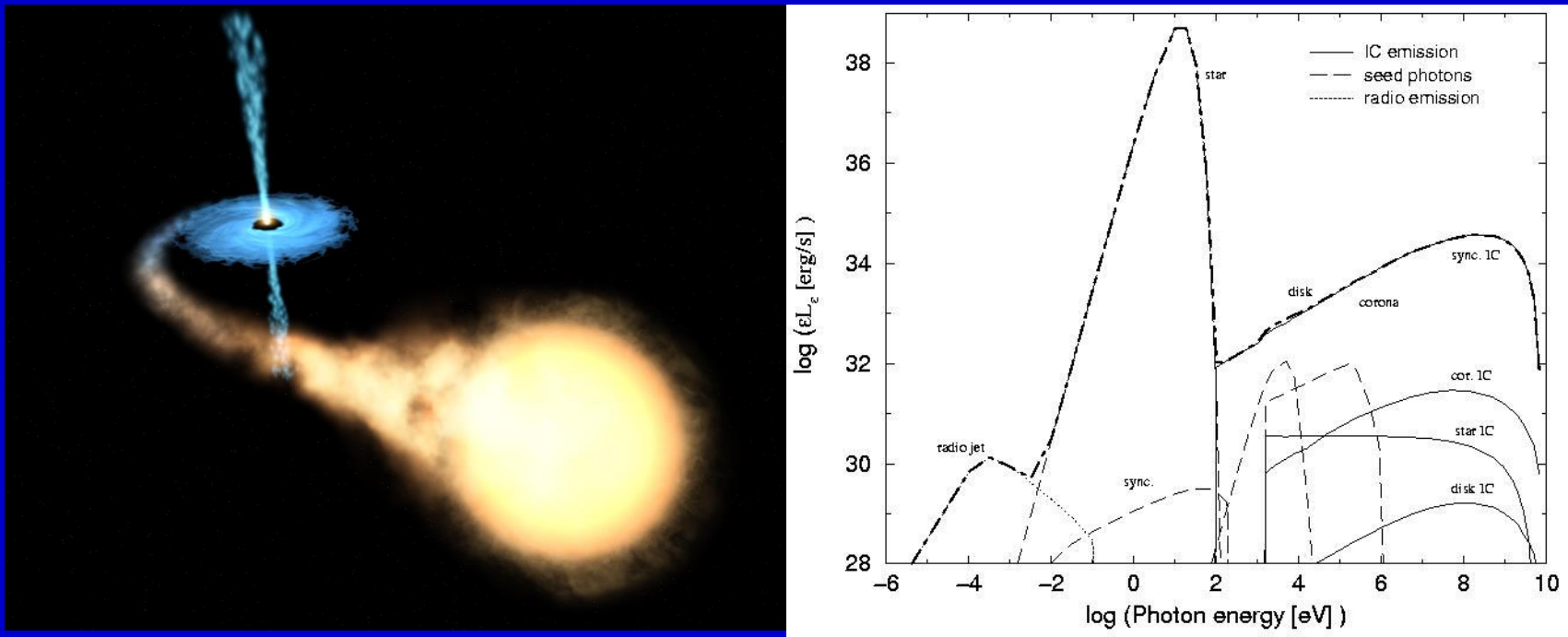
The jet length is ~ 1000 a.e.

Probably, the source was
observed by EGRET
as 3EG J1824-1514.

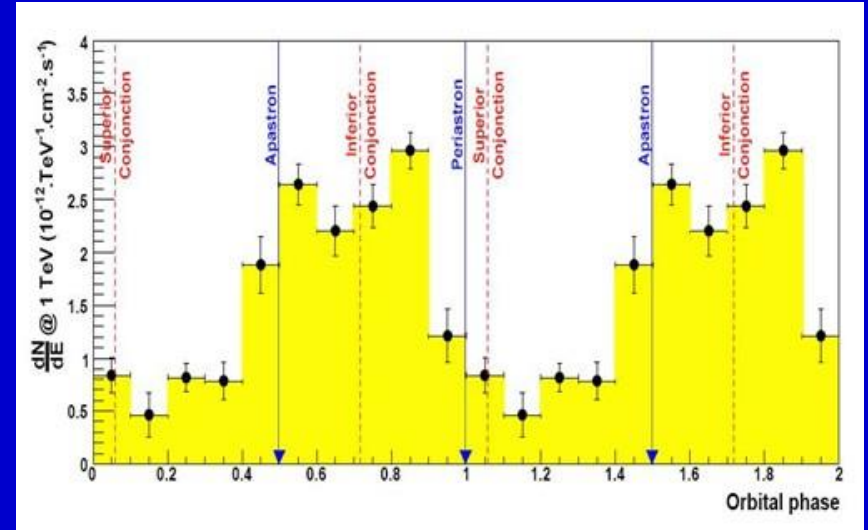
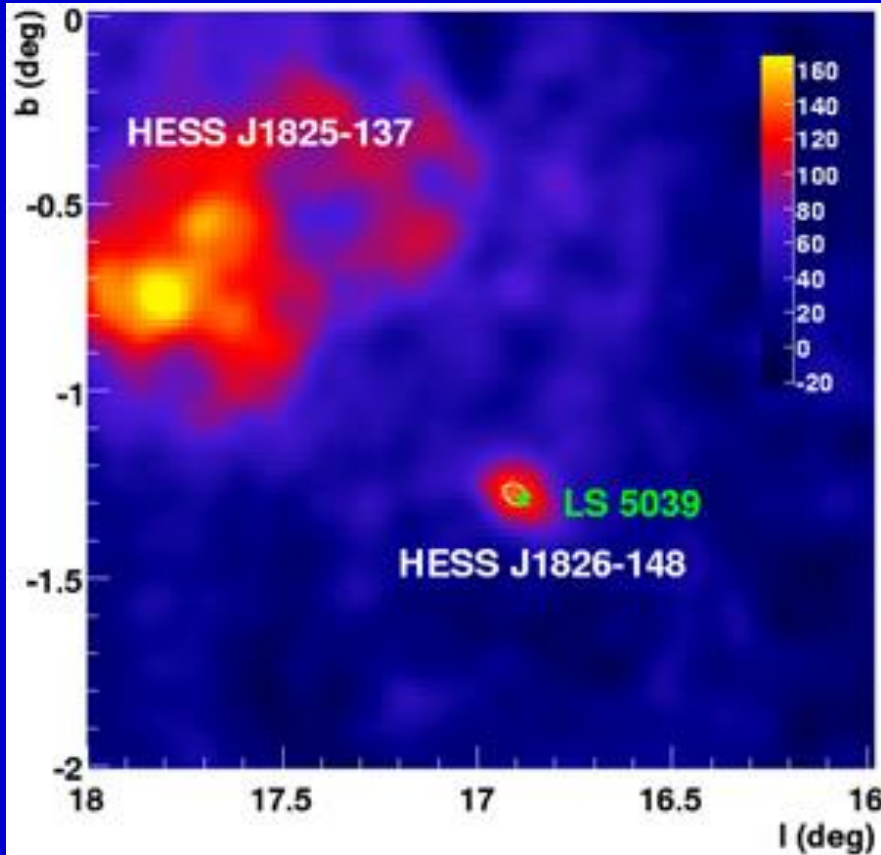
(Many examples of VLBI radio jets from different sources
can be found at the web-site <http://www.evlbi.org/gallery/images.html>)

The role of a donor

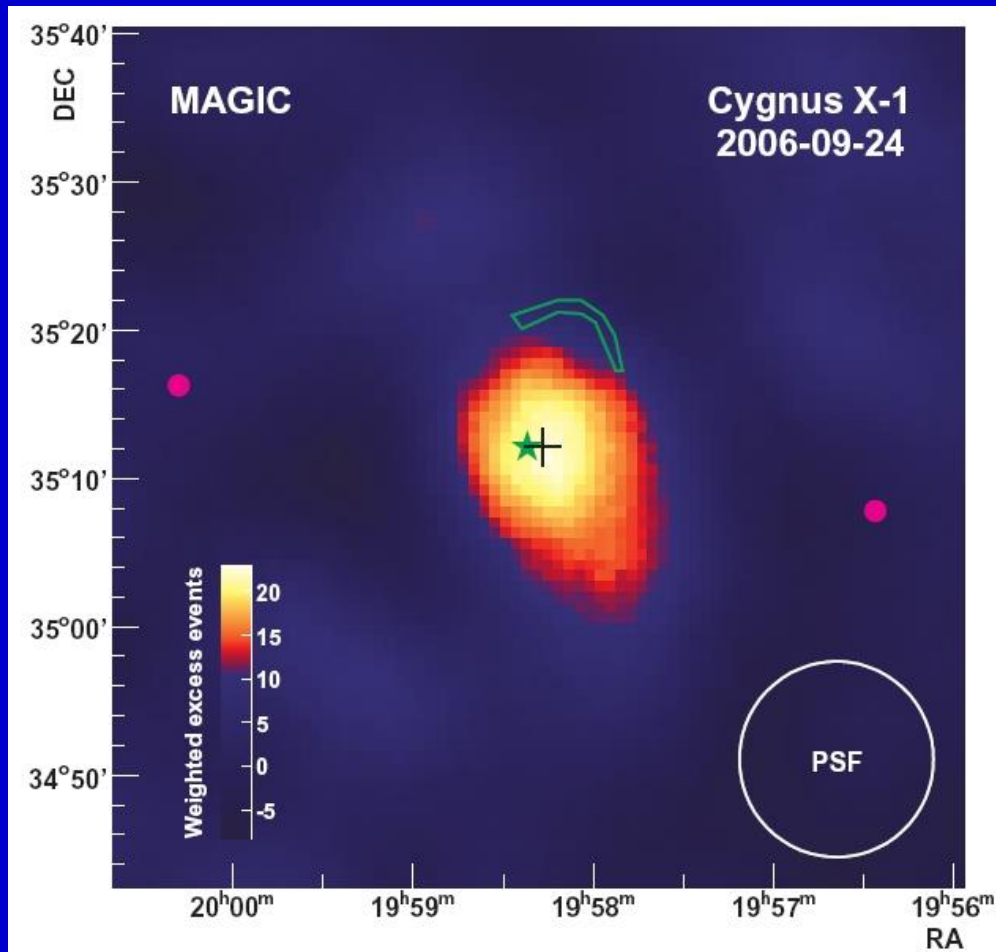
An important difference between the microquasars case and AGNs is related to the existence of a donor-star. Especially, if it is a giant, then the star can inject matter and photons into the jet.



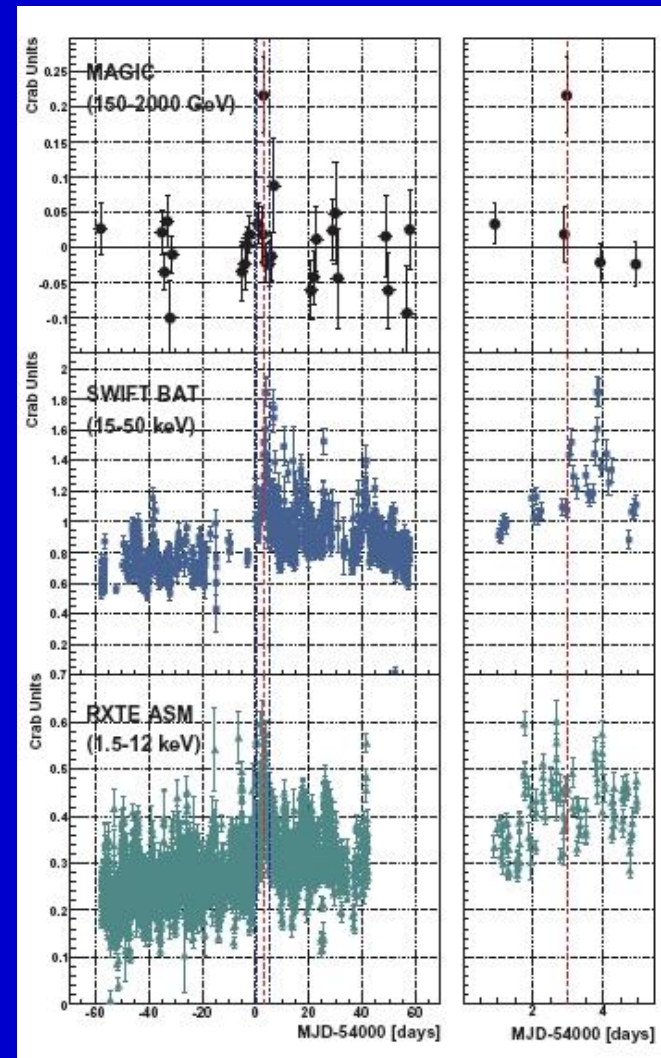
Microquasars in gamma-rays: TeV range



TeV emission from Cyg X-1



arxiv:0706.1505



See a review on jets in binaries in 1407.3674

Jet models

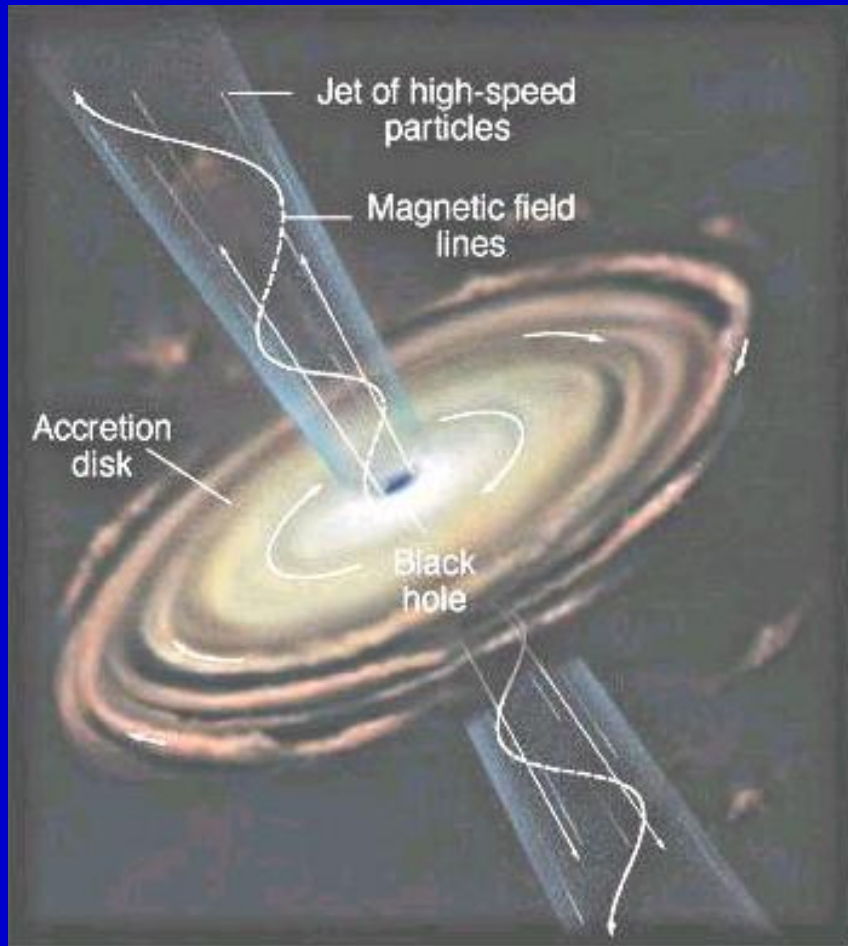


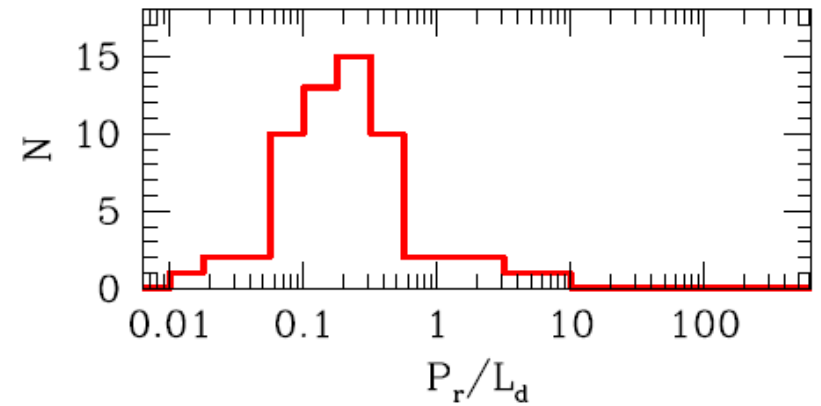
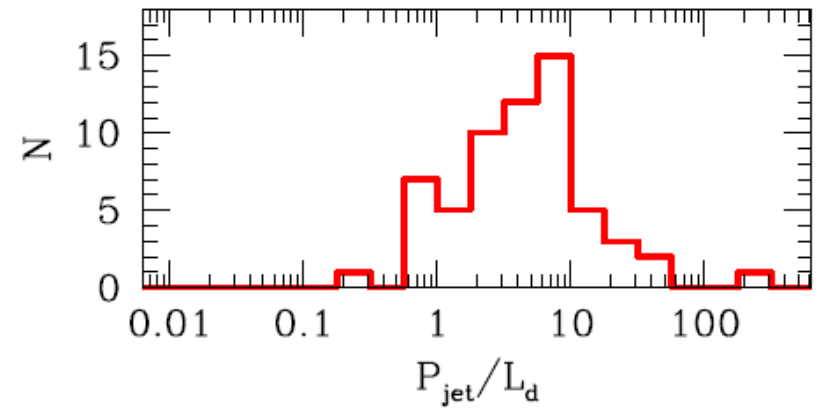
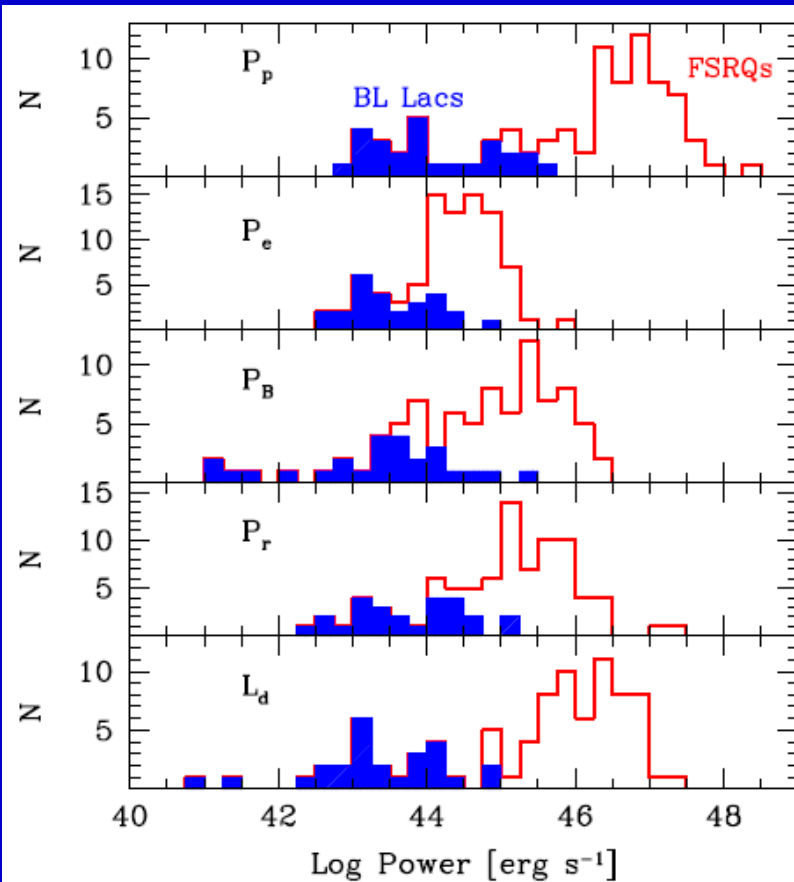
Table 1. Characteristic parameters of relativistic jet sources.

	L_j (erg/s)	Γ	Δt
GRB	10^{47} - 10^{50}	$10^2 - 10^3$	millisec - min.
AGN	10^{42} - 10^{47}	5 - 50	hours - years
MQ	10^{37} - 10^{40}	1 - 10	days
GF	10^{43} - 10^{46}	1	seconds

In all models jets are related to discs. Velocity at the base of a jet is about the parabolic (escape) velocity.

(the table is from astro-ph/0611521)

Jet power



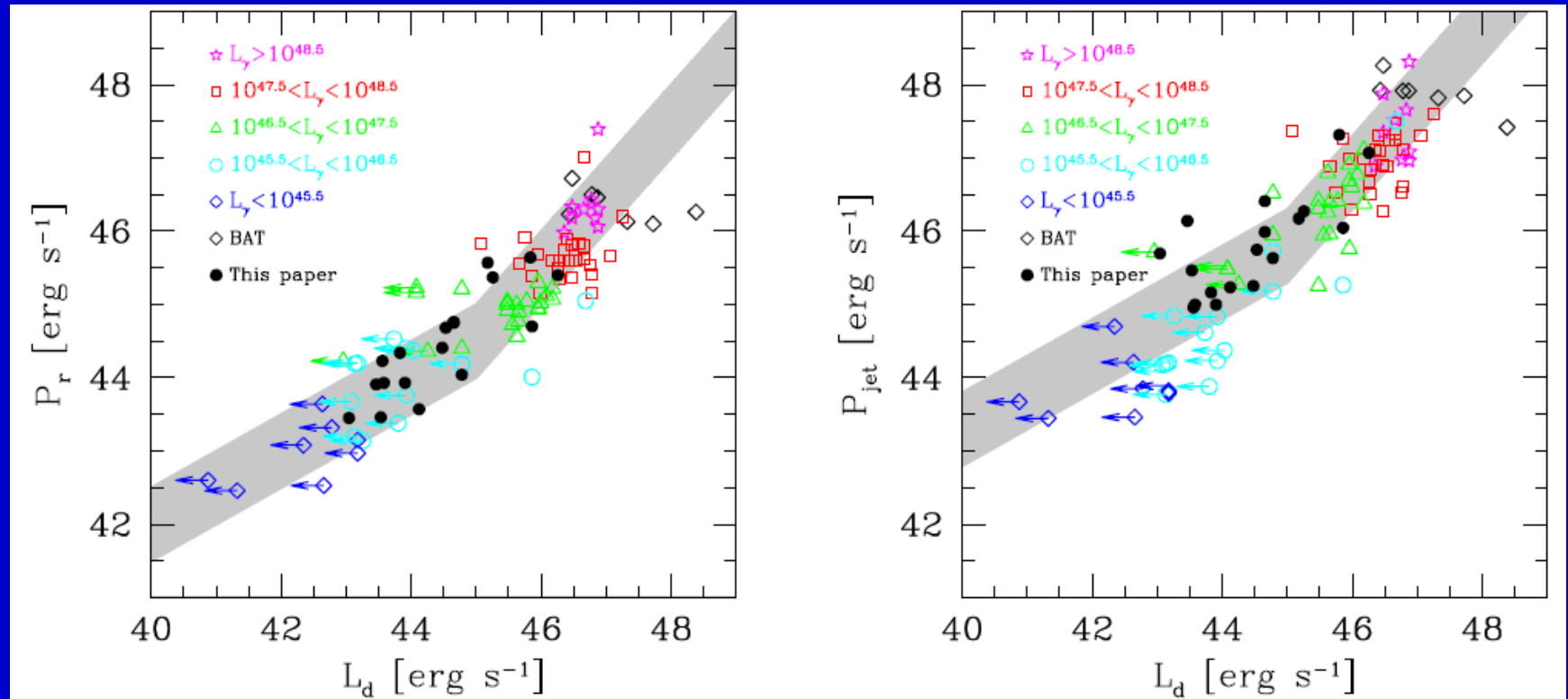
$$P_{\text{jet}} > 2P_r \sim 2L/\Gamma^2$$

Jet and disc

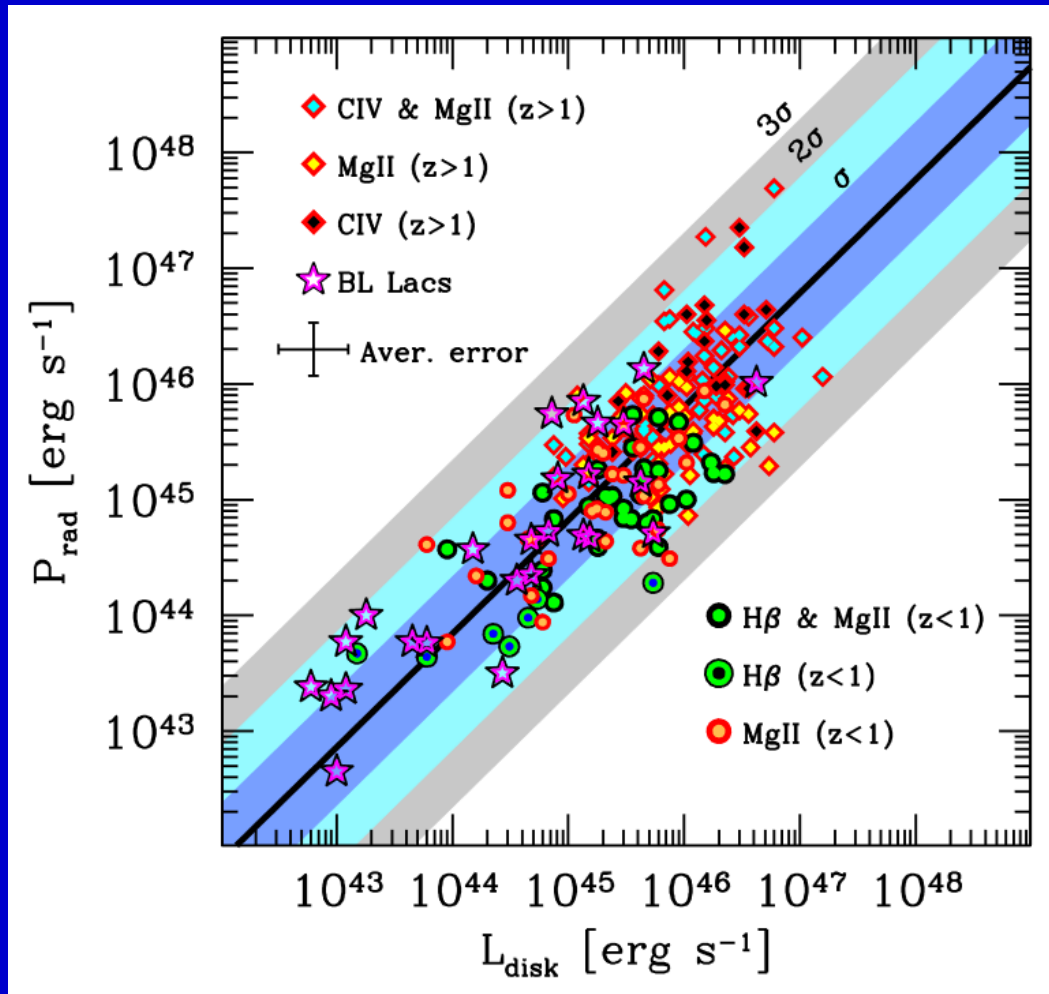
L_d – disc luminosity.

$$P_{\text{jet}} = P_B + P_P + P_e$$

In the gray stripes $P_{\text{jet}} \sim \dot{M}$ and
at low accretion rates $L_d \sim \dot{M}^2$, at large - $L_d \sim \dot{M}$.

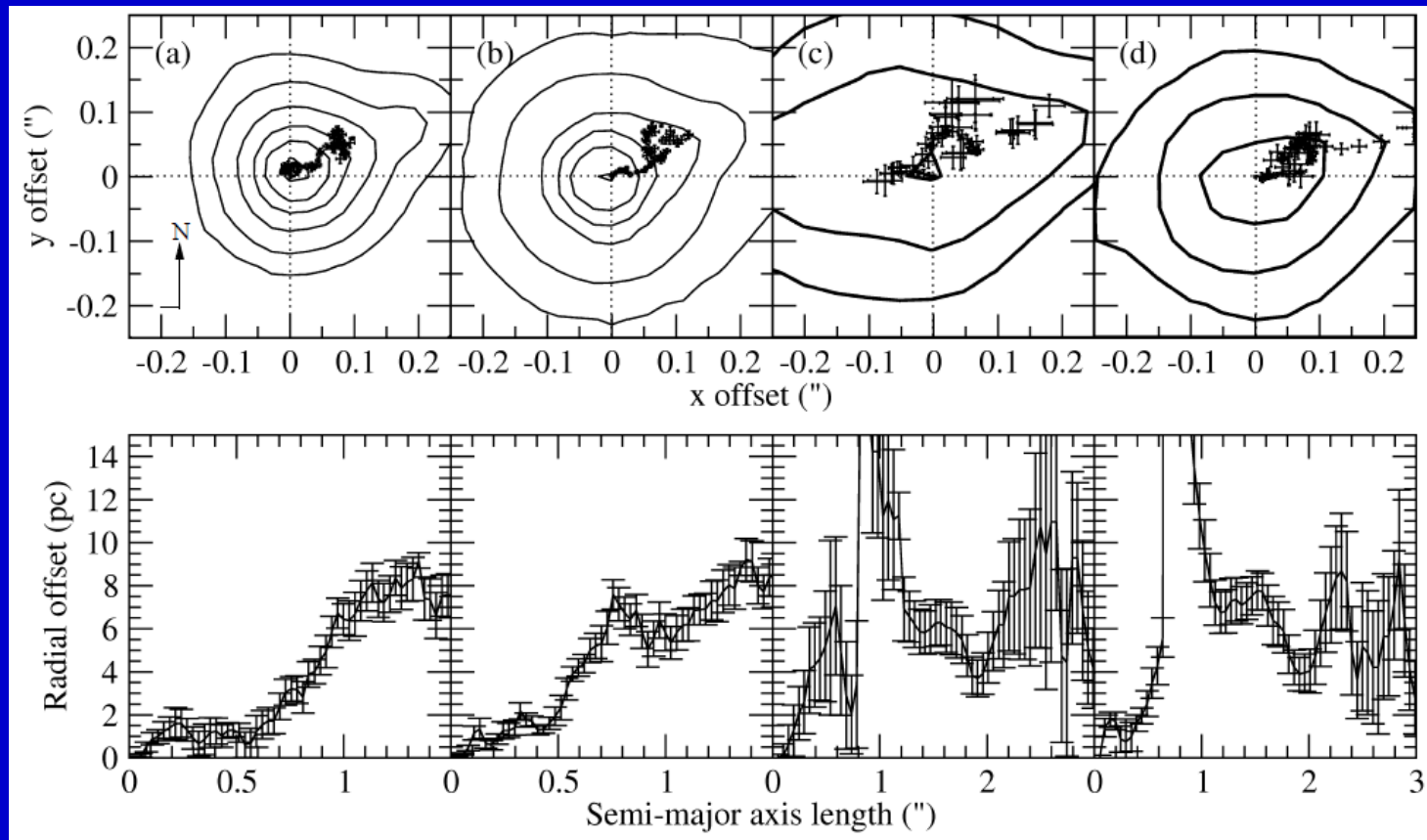


Jets are more powerful than discs

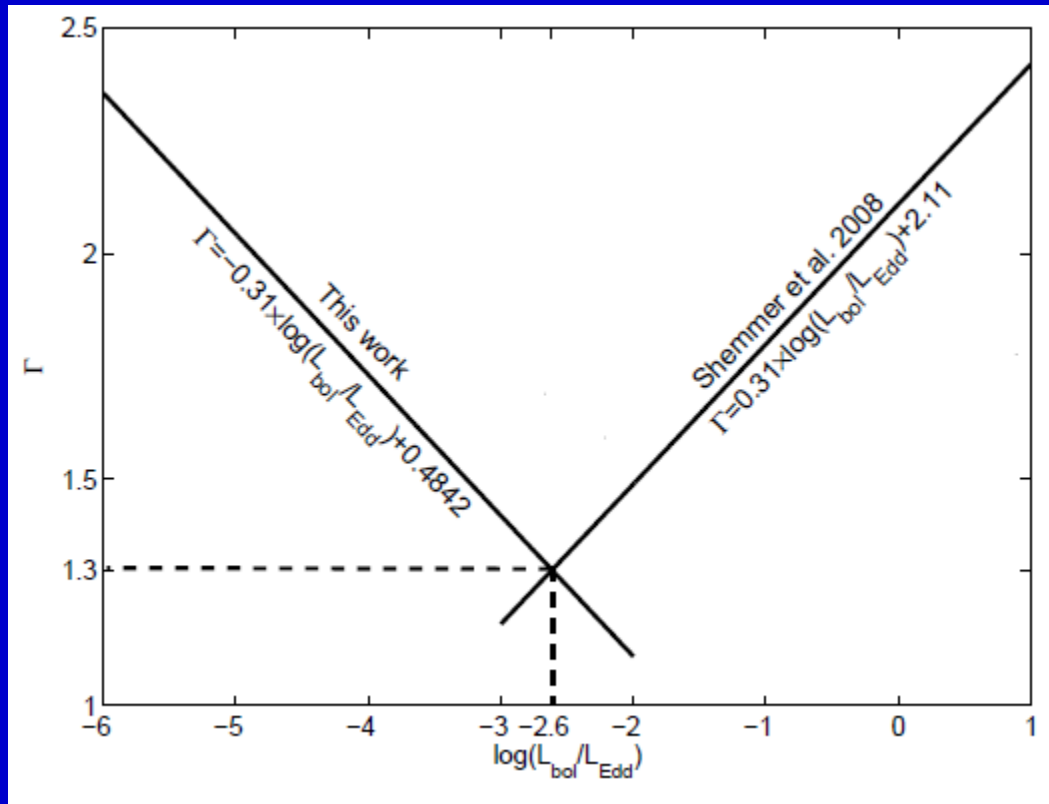


Displaced SMBH in M87

Projected displacement of 6.8 ± 0.8 pc
consistent with the jet axis
displaced in the counter-jet direction



Different accretion regimes in AGNs



Γ - photon index

Anticorrelation for low-luminosity AGNs (LINERS).

Correlation for luminous AGNs.

In the critical point the accretion regime can be changed: from a standard thin accretion disc to RIAF (radiatively inefficient accretion flow).

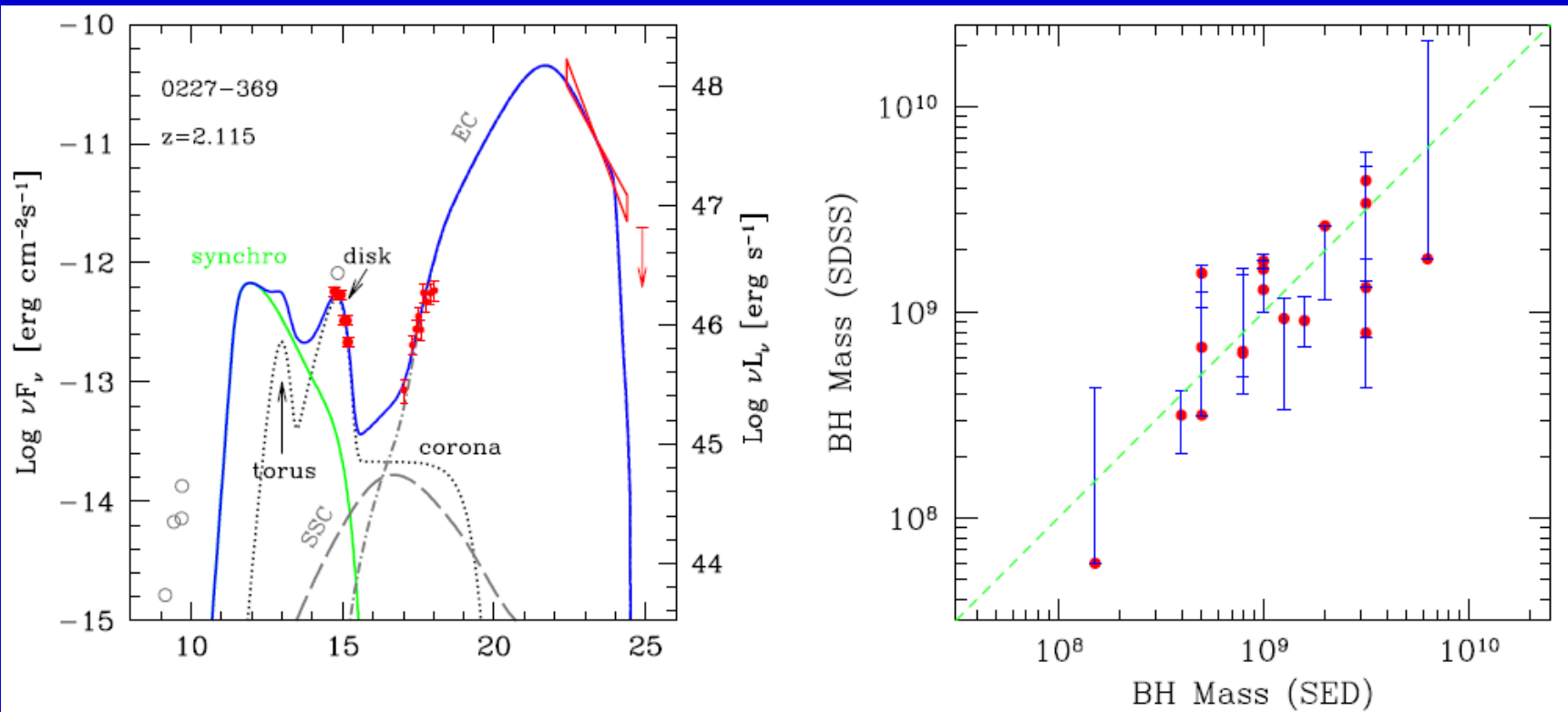
BH mass determination

Accretion disc contribution is visible in opt-UV.

It allows to estimate the BH mass.

It can be compared with emission lines estimates.

Bars correspond to different lines used.



BH mass and jet properties in M87

Table 3. Predicted jet and BH parameters for $M = 6.5 \times 10^9 M_{\odot}$.

σ_M	$\Gamma\theta_j$	ϕ	a_*	W_j (10^{42} erg/s)
(1)	(2)	(3)	(4)	(5)
10	0.062	3.2	0.093	1.9
20	0.063	3.3	0.144	4.7

Estimates are in correspondence with the EHT data on the BH mass.

If the mass is assumed to be known,
then the initial magnetization σ_M can be determined.

Tidal disruption

The Hills limit: 3×10^8 solar masses. A BH disrupts stars.

After a disruption in

$$(t_0 - t_D) \sim 1.1 M_8^{1/2} \text{ yr}$$

happens a burst with
the temperature

$$T_{\text{eff}} \approx (L_{\text{Edd}}/4\pi\sigma R_T^2)^{1/4} = 3.7 \times 10^5 M_8^{1/12} \text{ K}$$

The maximum accretion rate

$$\dot{M}_{\text{max}} \sim 0.14 M_8^{1/2} M_{\odot} \text{ yr}^{-1}$$

This rate corresponds to the moment

$$(t_{\text{max}} - t_D) \sim 1.5 (t_0 - t_D)$$

Then the rate can be described as

$$\dot{M}(t) = 0.3 M_8 [(t - t_D)/(t_0 - t_D)]^{-5/3} M_{\odot}$$

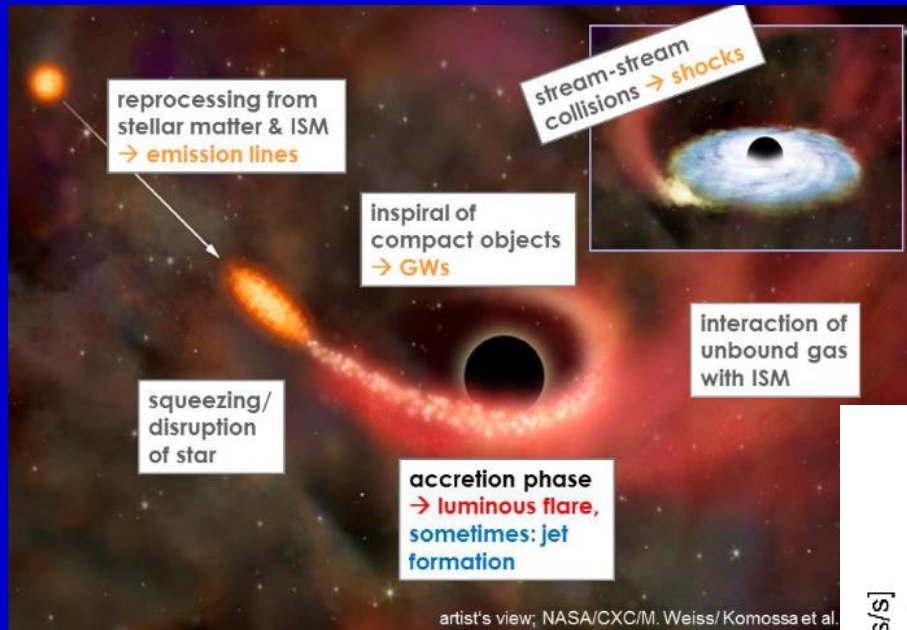
For a BH with $M < 10^7 M_{\odot}$ the luminosity at maximum is:

$$L_{\text{flare}} \geq \eta \dot{M}_{\text{Edd}} c^2 > 1.3 \times 10^{45} M_7 \text{ ergs s}^{-1}$$

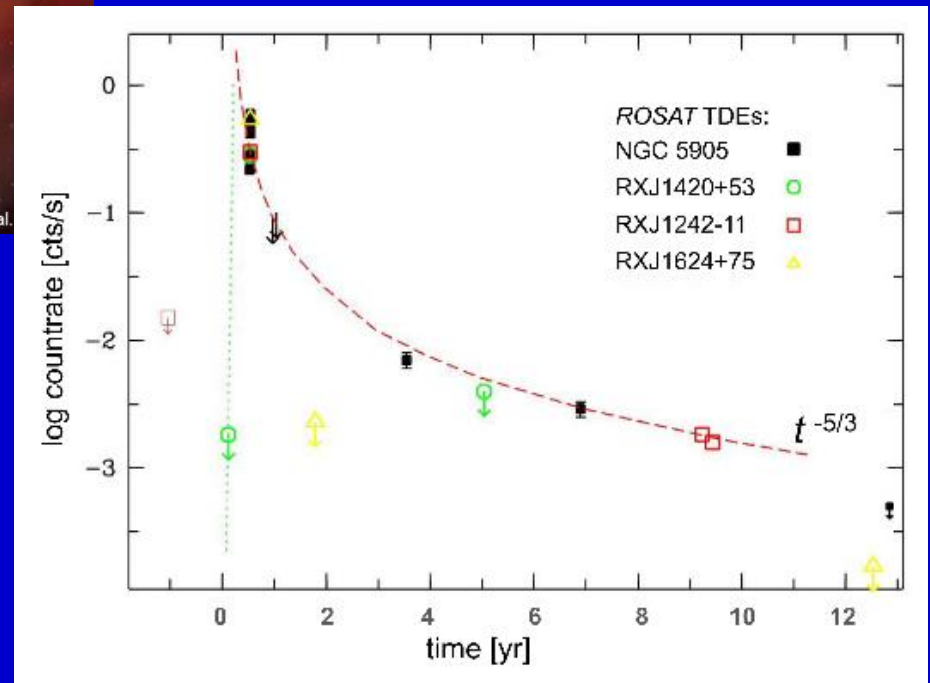
(astro-ph/0402497)

See a review in 1505.01093

General picture

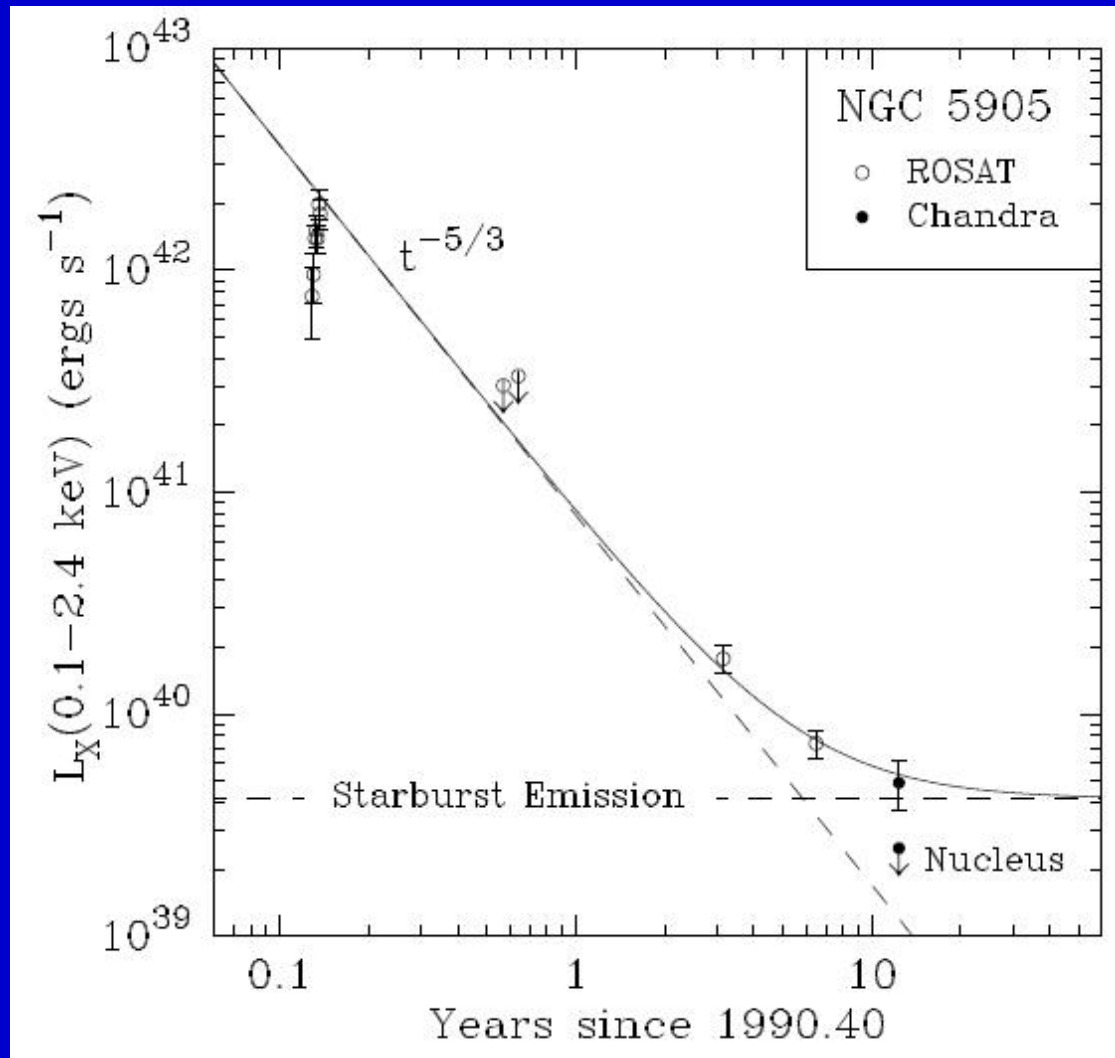


Rate of TDE is $\sim 1/100000$ yrs per galaxy (1407.6425).



See a review in 1505.01093

A burst in NGC 5905



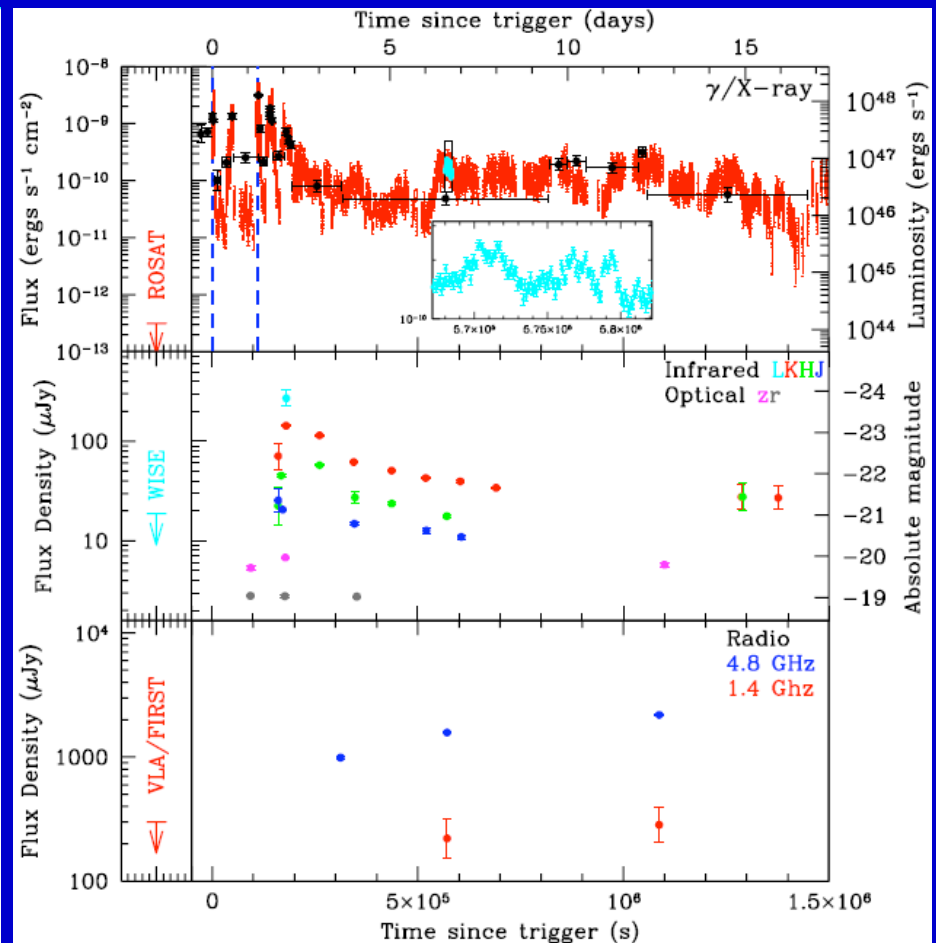
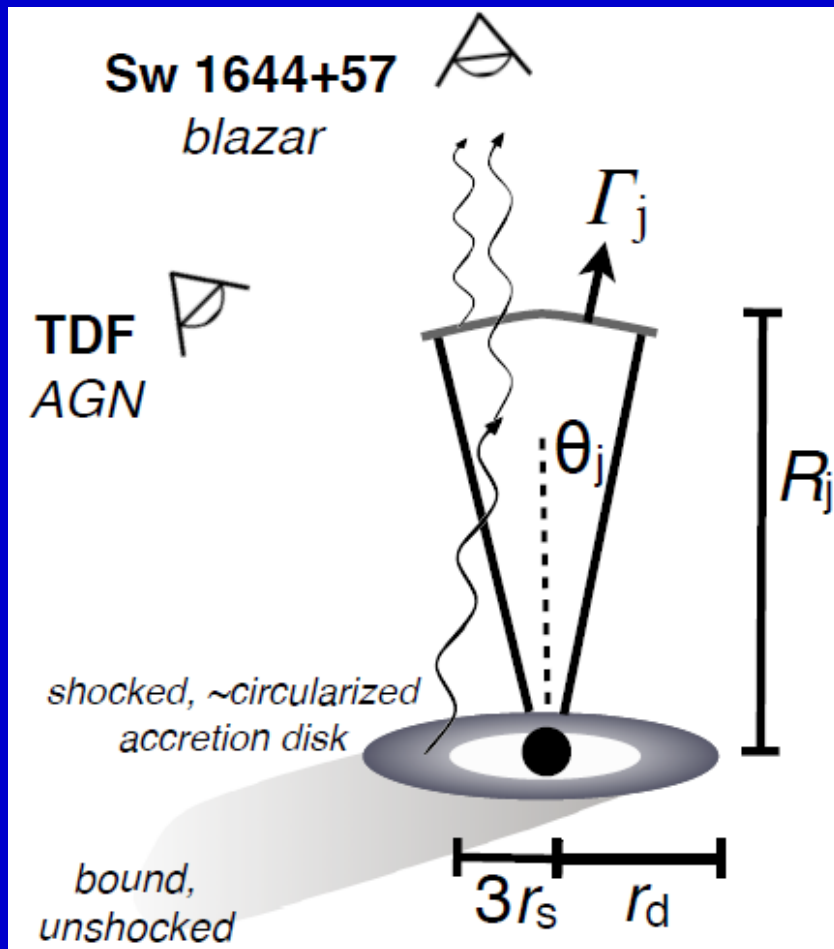
The decay was well described by the relation:

$$(t - t_D)^{-5/3}$$

Two other bursts discovered by ROSAT and observed by HST and Chandra:

RX J1624.9+7554
RX J1242.6-1119A

High-energy transient Swift J164449.3+573451

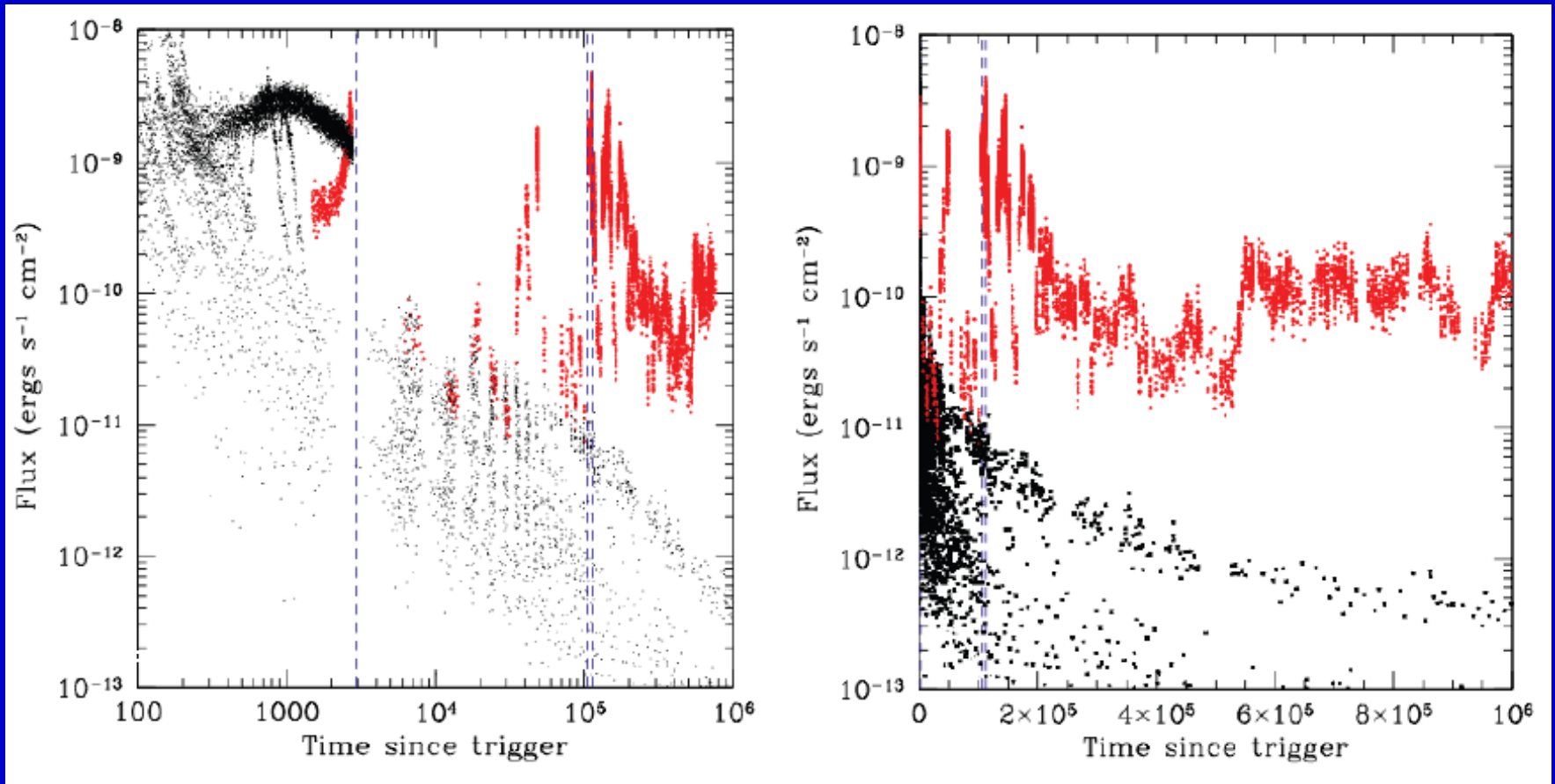


1104.3257

1104.3356

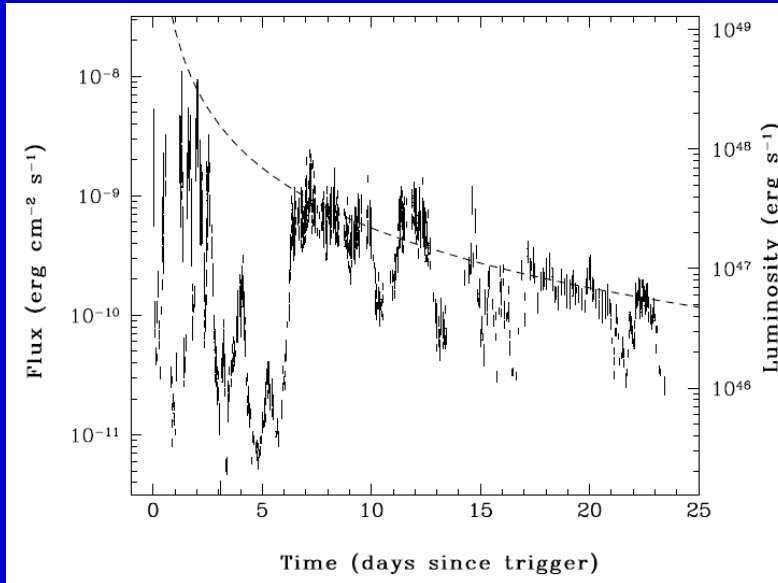
Also known as GRB 110328A

A unique event

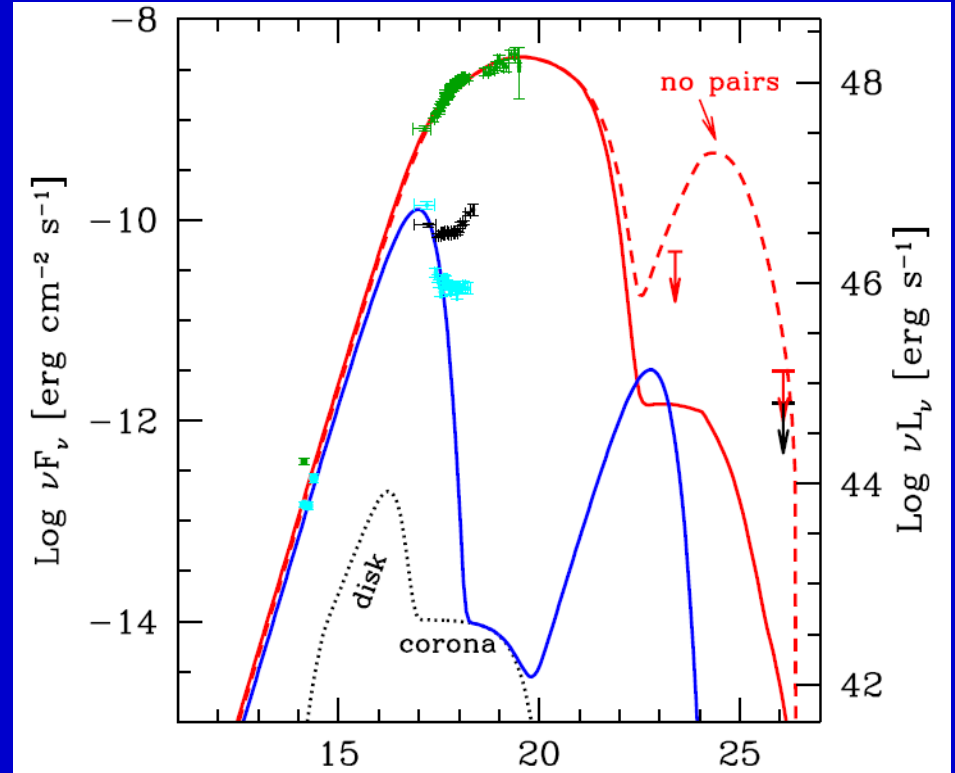


The transient does not look similar to GRBs, SN or any other type of event

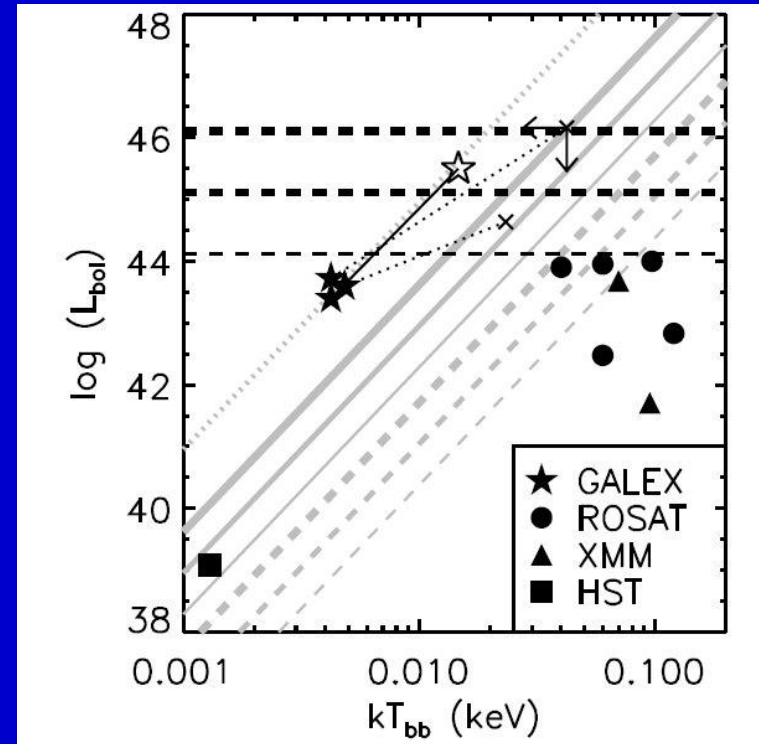
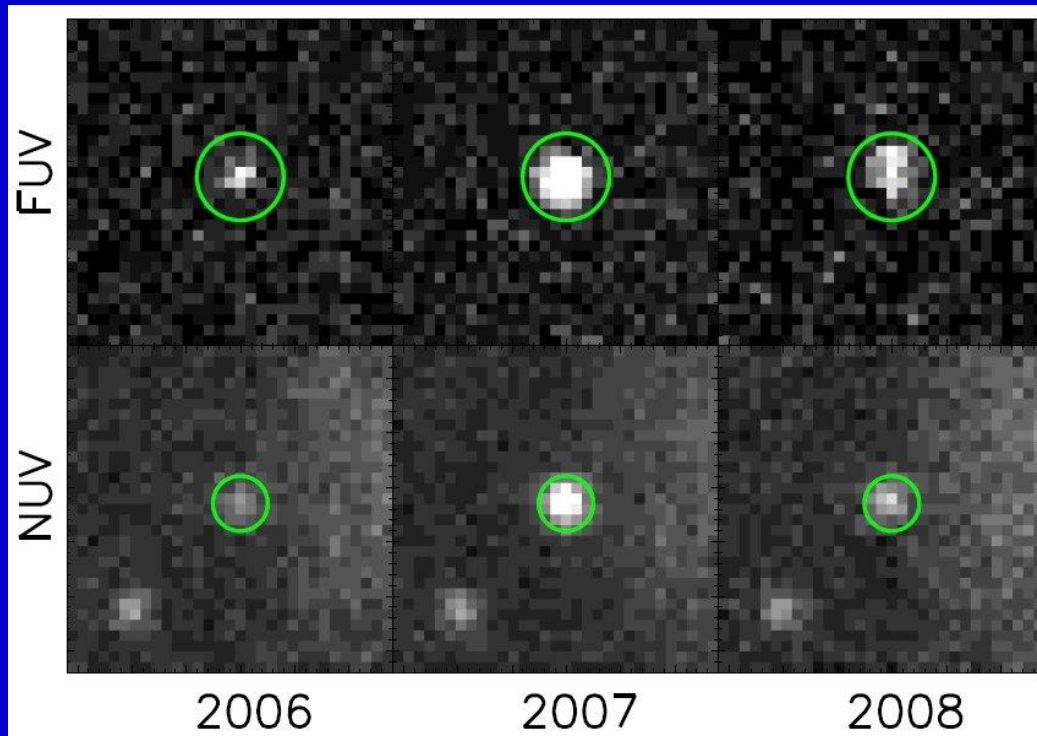
A tidal disruption event



Light curve fits the prediction
for a tidal event.
The spectrum is blazar-like.



Optical observations of tidal disruptions



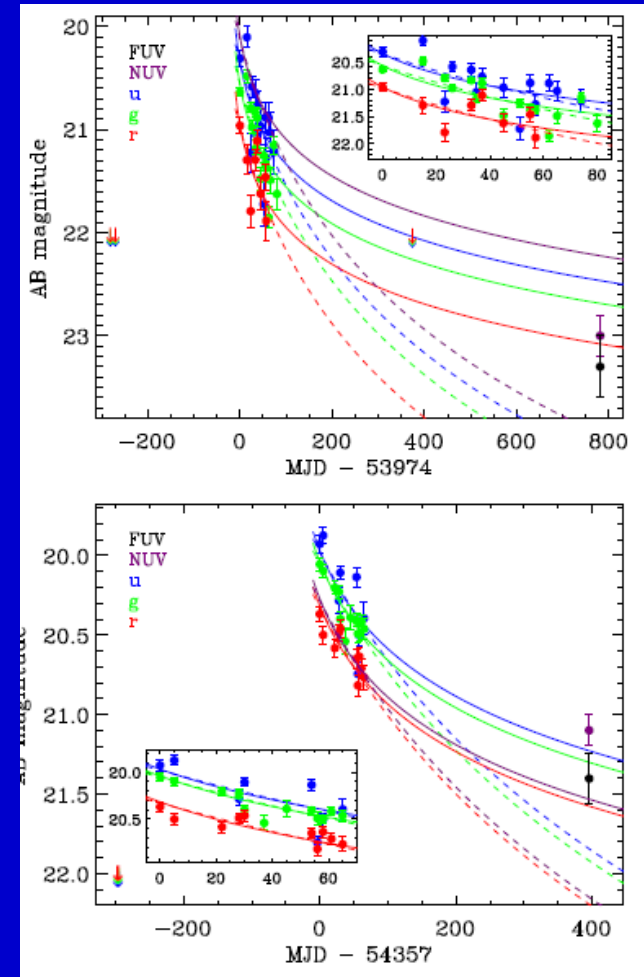
In optics one can observe events far from the horizon.
Future surveys (like Pan-STARRS)
can discover 20-30 events per year.

Two more examples of optical flares due to tidal disruption events

SDSS data

Atypical flares

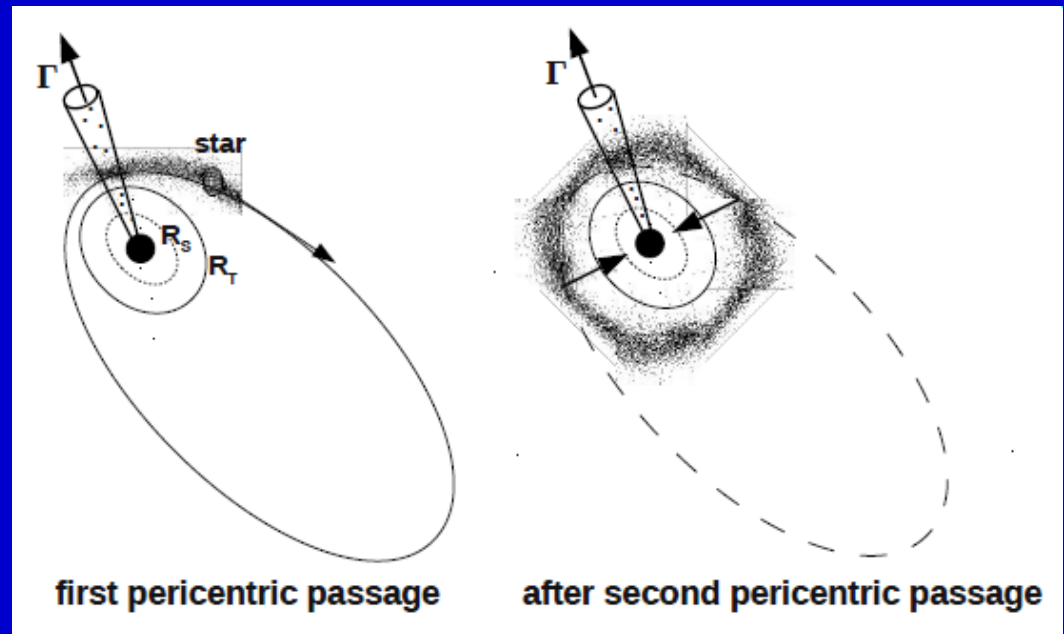
Rate estimates:
 $\sim 10^{-5}$ per year per galaxy
or slightly more



Theoretical models

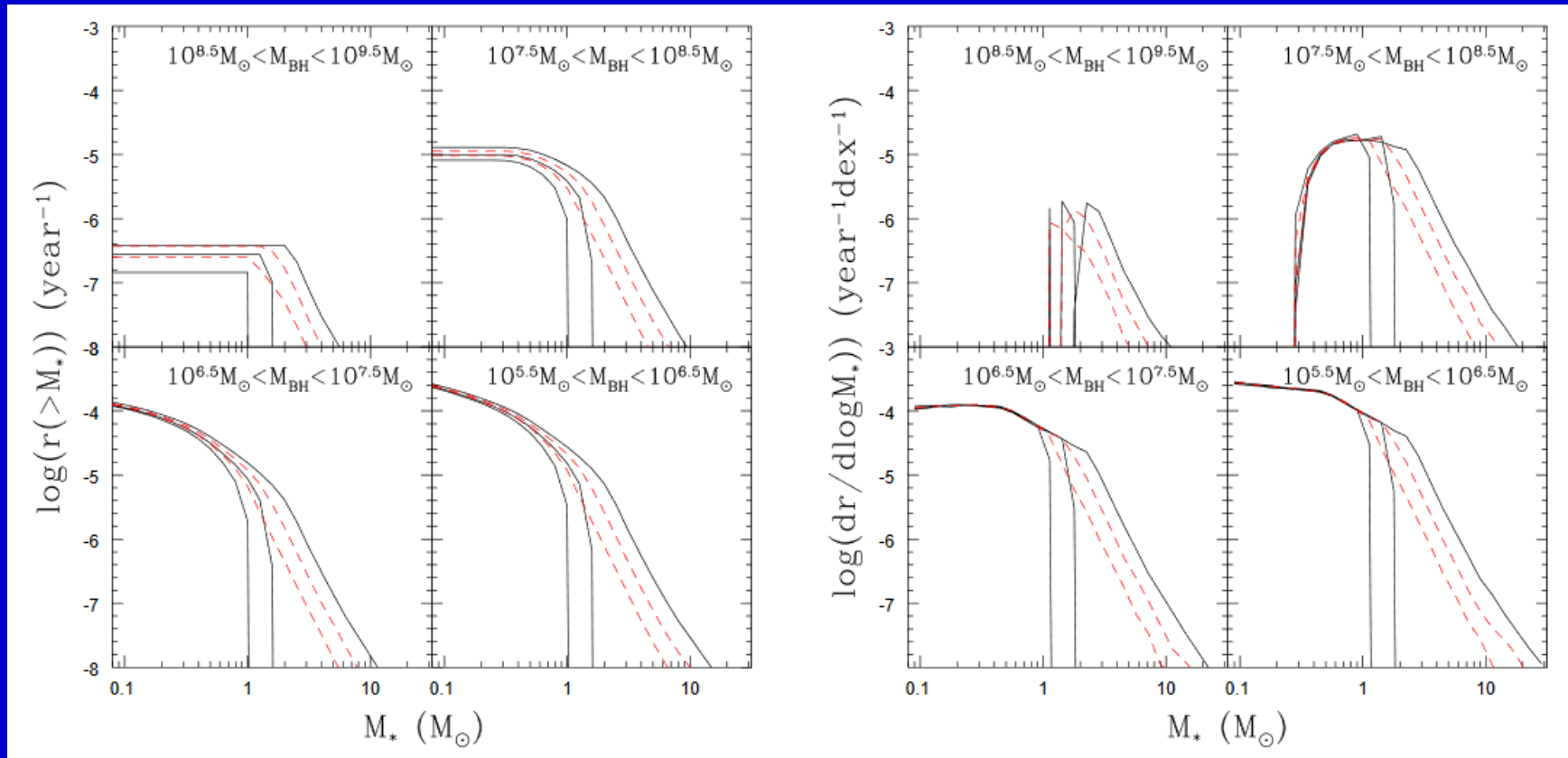
- X-rays. 1105.2060
- Radio. 1104.4105

Flows of hot X-ray emitting gas have been identified after one of tidal disruption events.
1510.06348



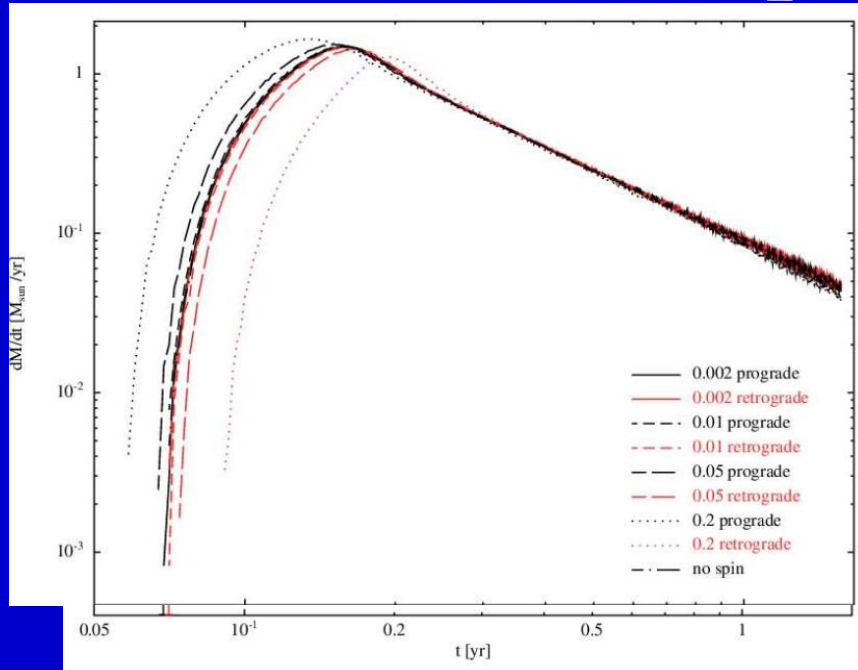
1104.2528

Stellar masses

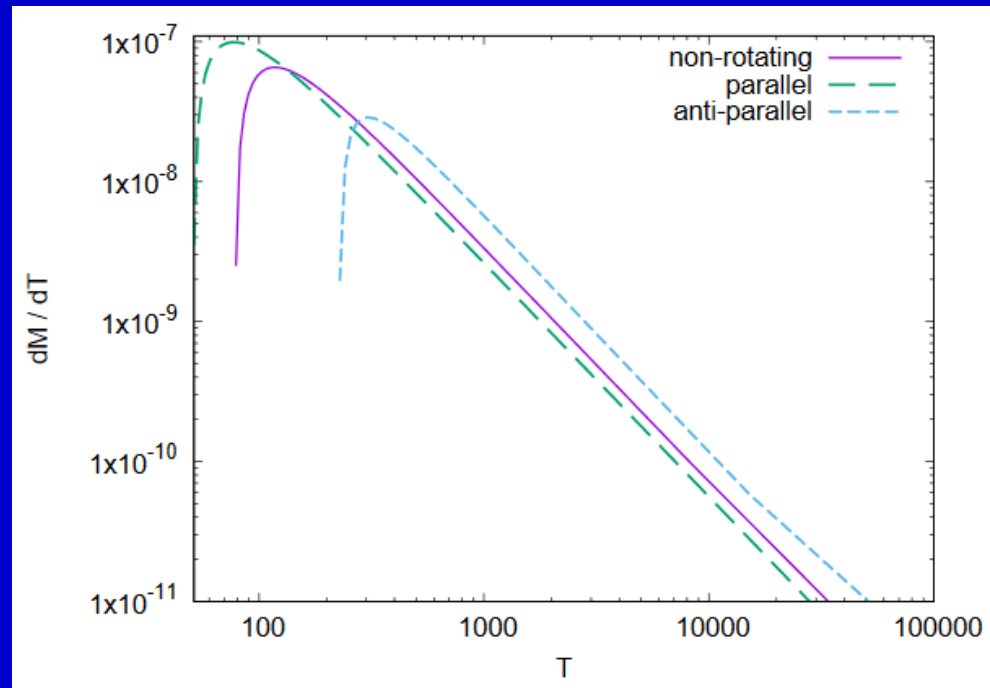


For not too massive BHs the main contribution is due to M-dwarfs ($0.3M_{\text{solar}}$).
For massive BHs contribution from massive and evolved stars grows.

Role of stellar spin



1901.03717



1901.05644

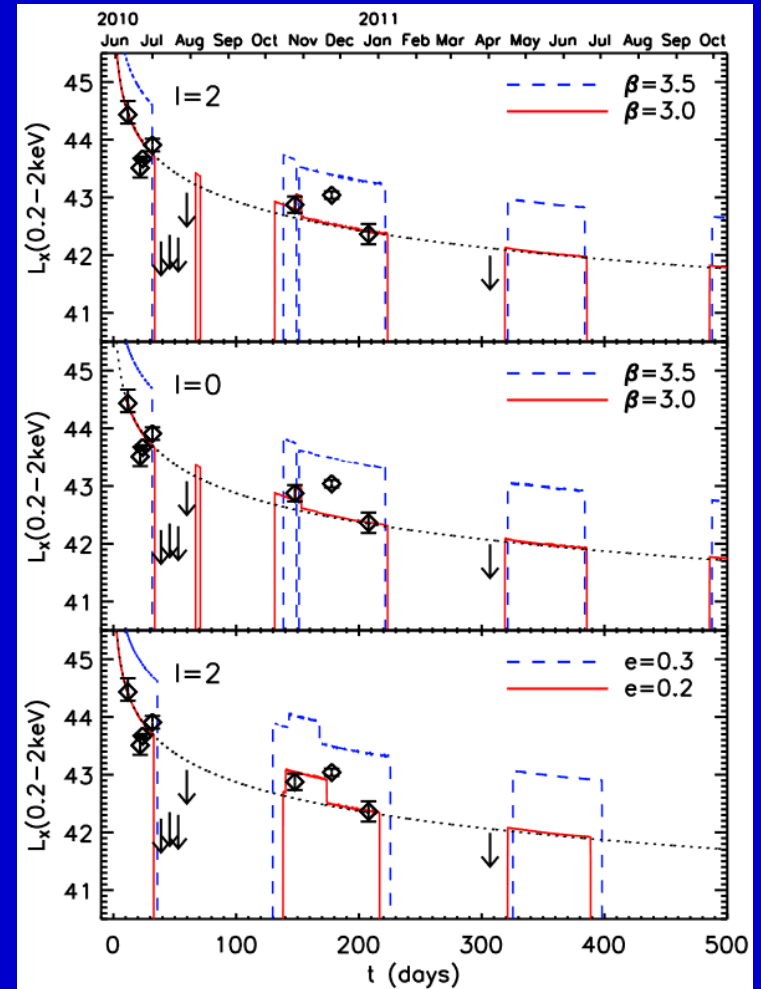
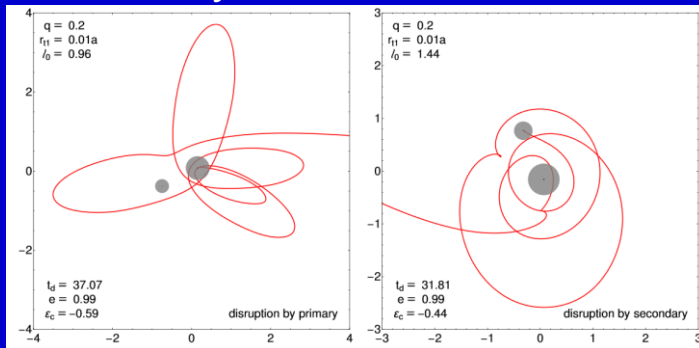
TDE and binary SMBHs

It has been predicted that after a TDE in a system of close SMBH binary there might be particular drops in the light curve. Such phenomena was observed.

SDSS J120136.02+300305.5
XMM-Newton observations

Masses $\sim 10^7$ and 10^6 solar masses,
orbital separation $\sim 10^{-3}$ pc
Eccentricity ~ 0.3

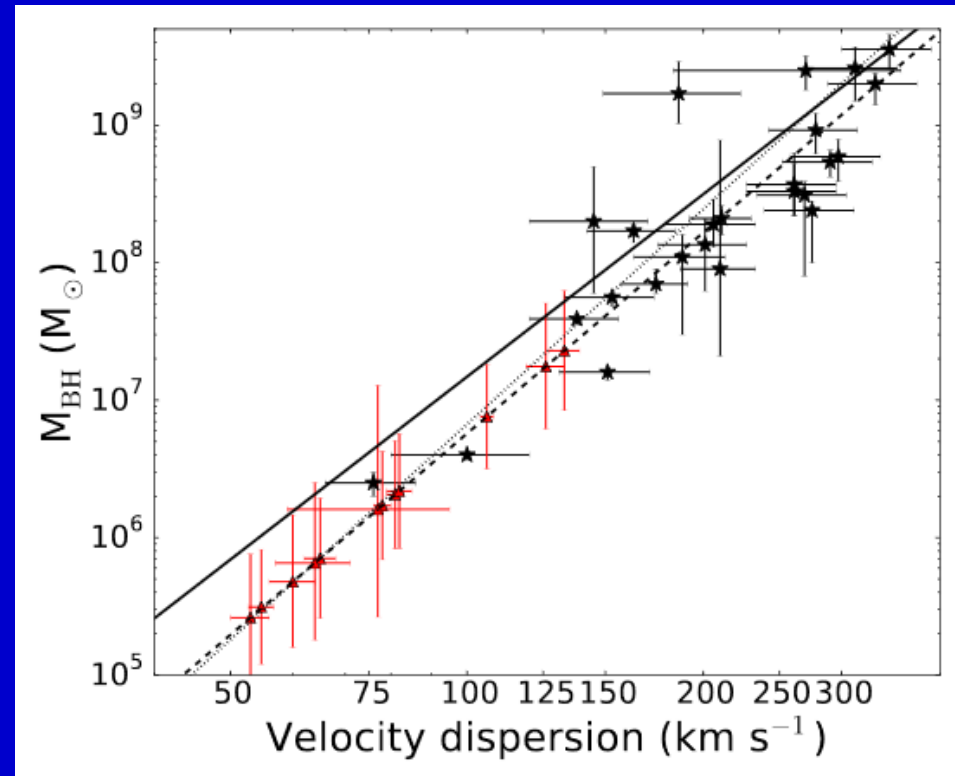
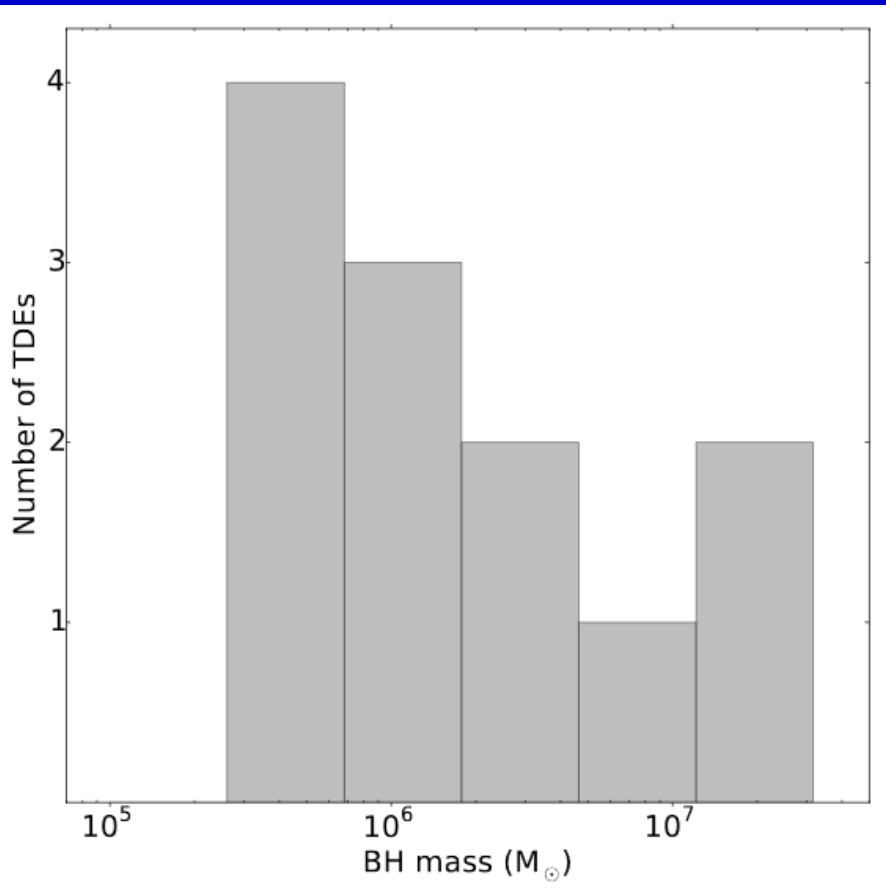
TDEs in supermassive BH binaries
were recently modeled in 1802.07850.



1404.4933

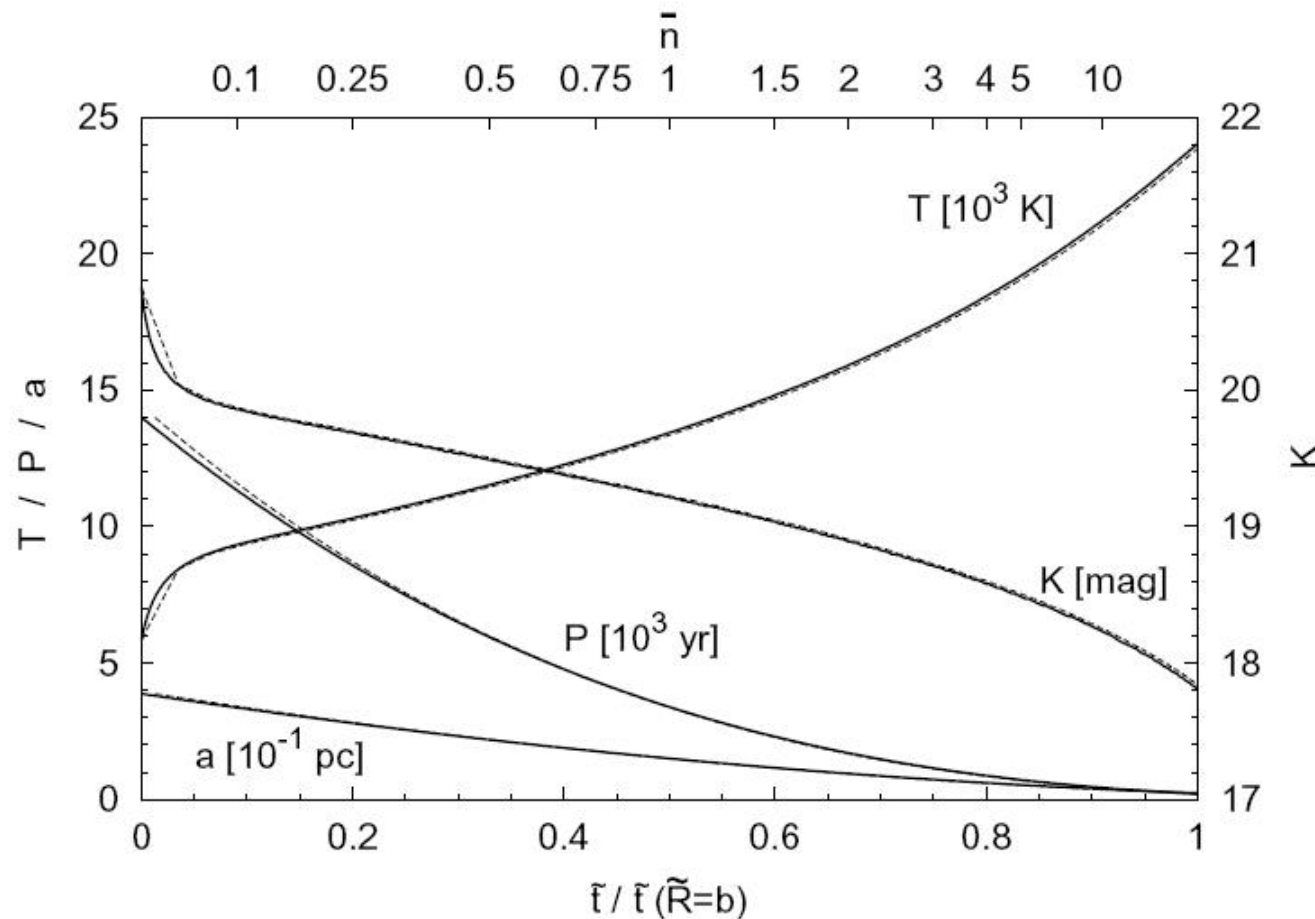
Mass determination from TDE

12 optically/UV selected TDE host galaxies



Red- new data, lines – best fits,
black – Ferrarese, Ford (2005).

Squeezars



The rate of formation is lower than the rate of tidal disruption events, but the observable time is longer.

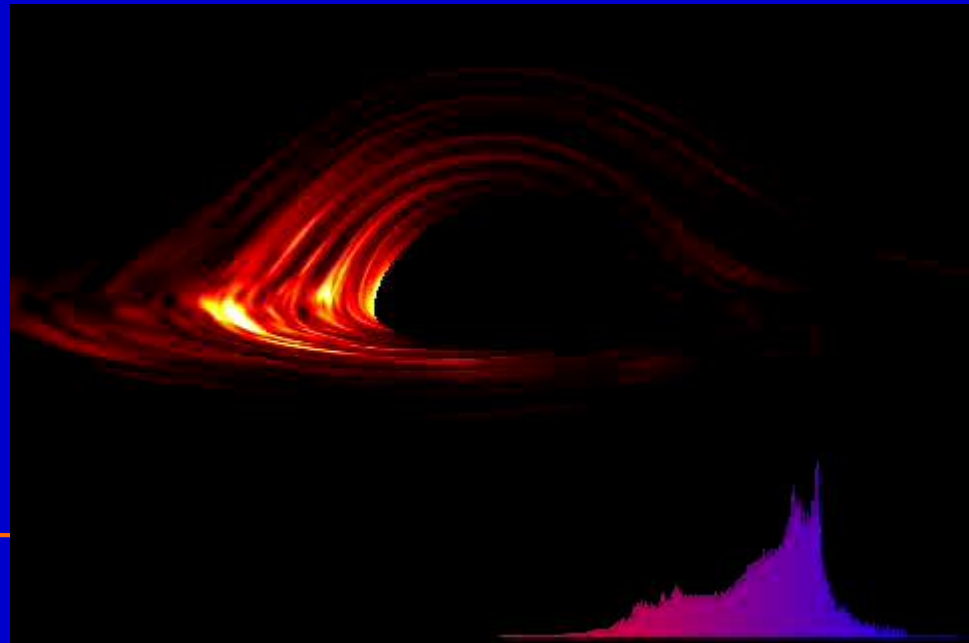
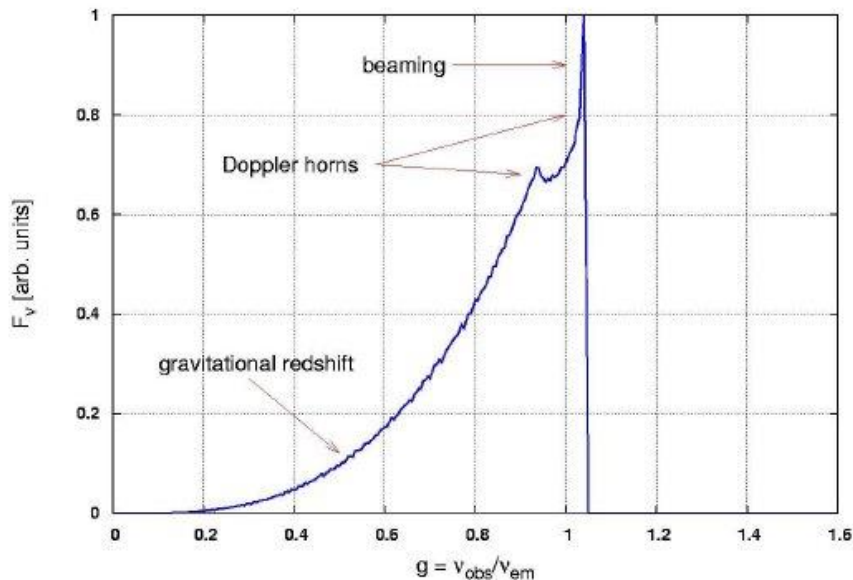
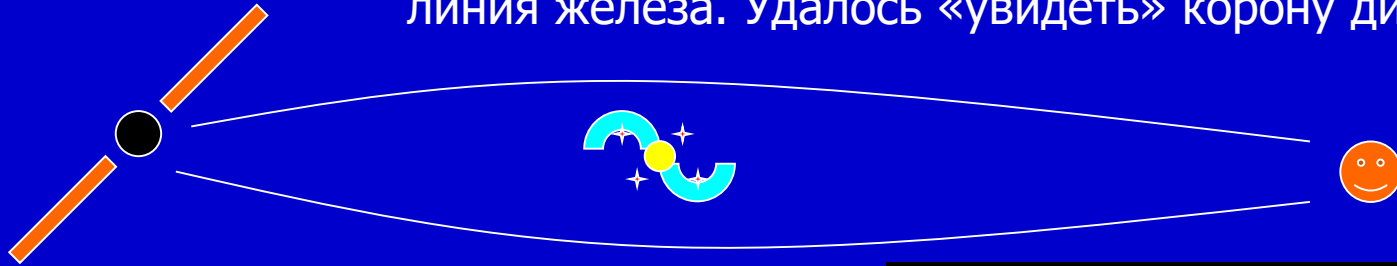
Graphs are plotted for a solar-type star orbiting the BH in the center of our Galaxy.

(astro-ph/0305061)

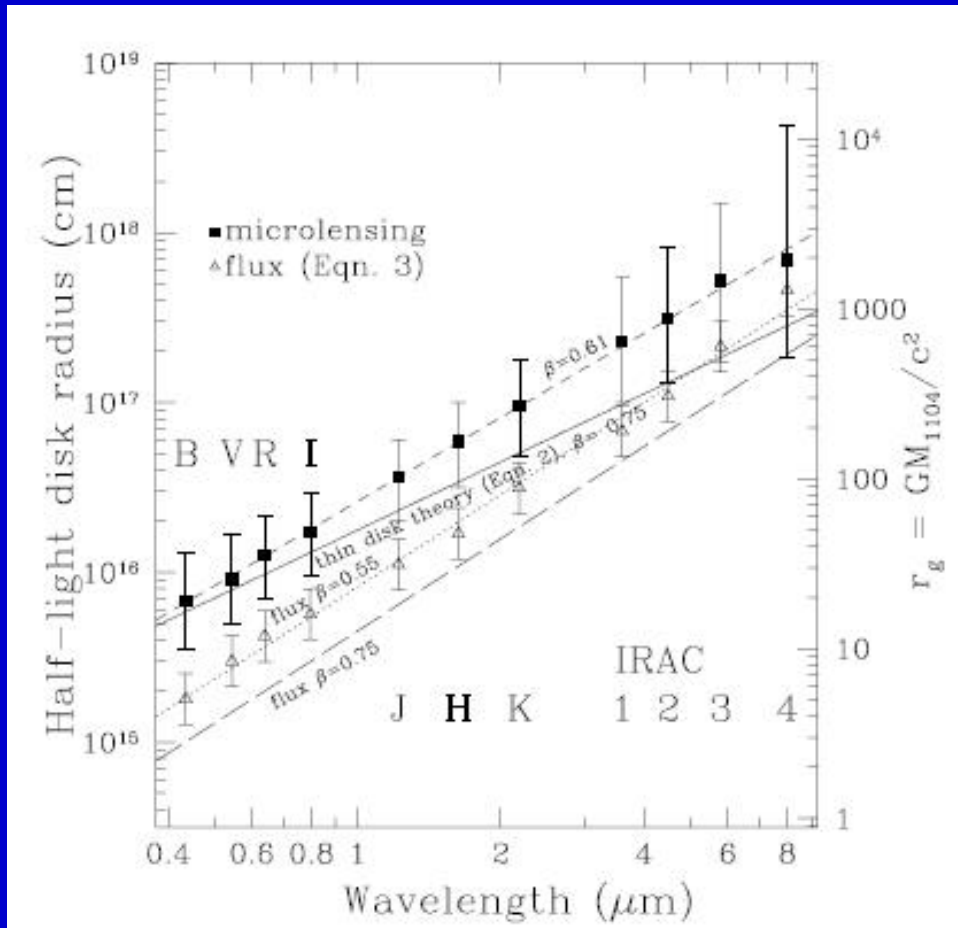
Структура диска вокруг сверхмассивной черной дыры

Наблюдение микролинзирования позволяет
выявлять структуру аккреционного диска.
Кроме этого, наблюдалась линзированная
линия железа. Удалось «увидеть» корону диска.

1204.4480

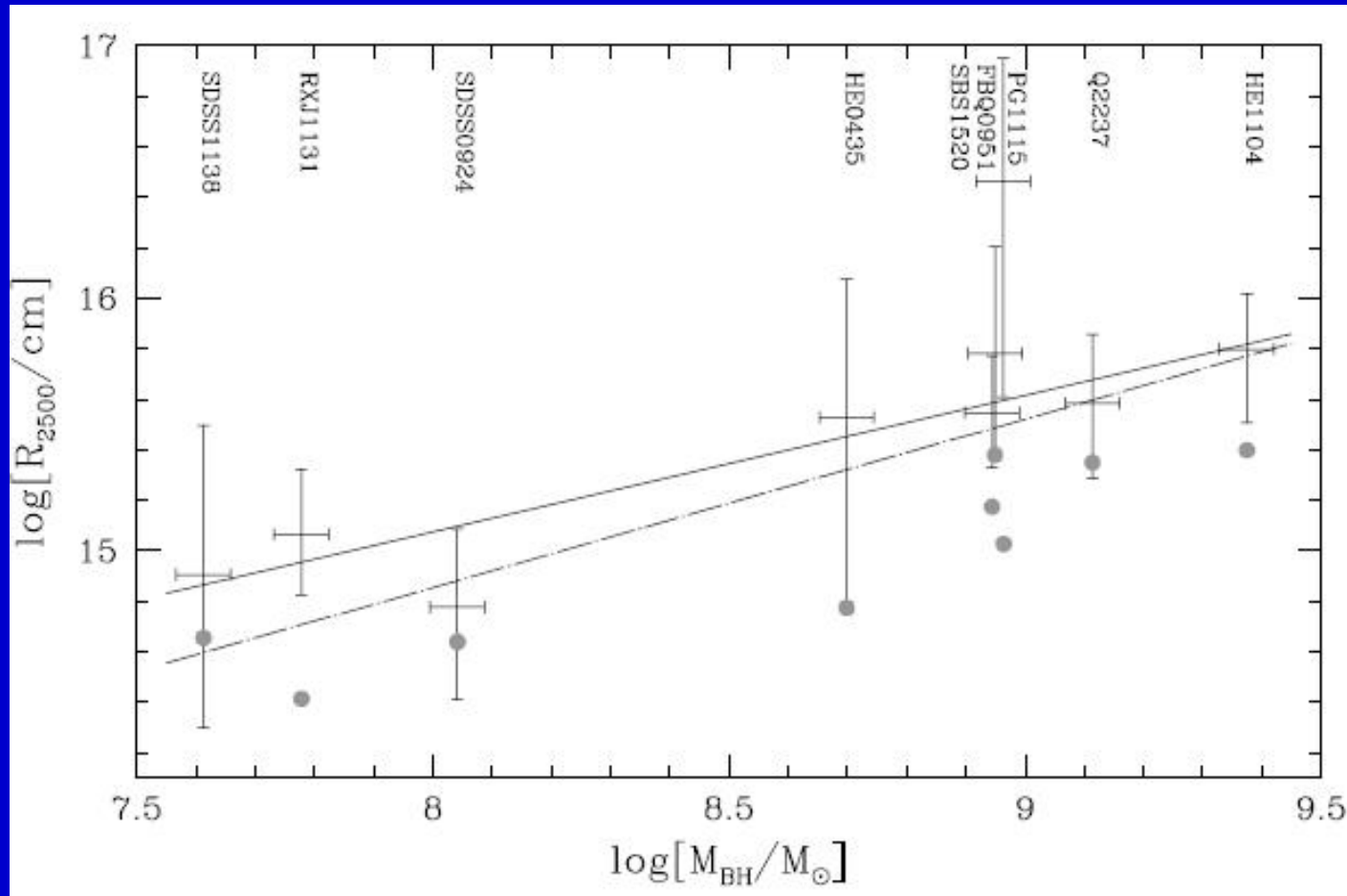


Disc structure from microlensing



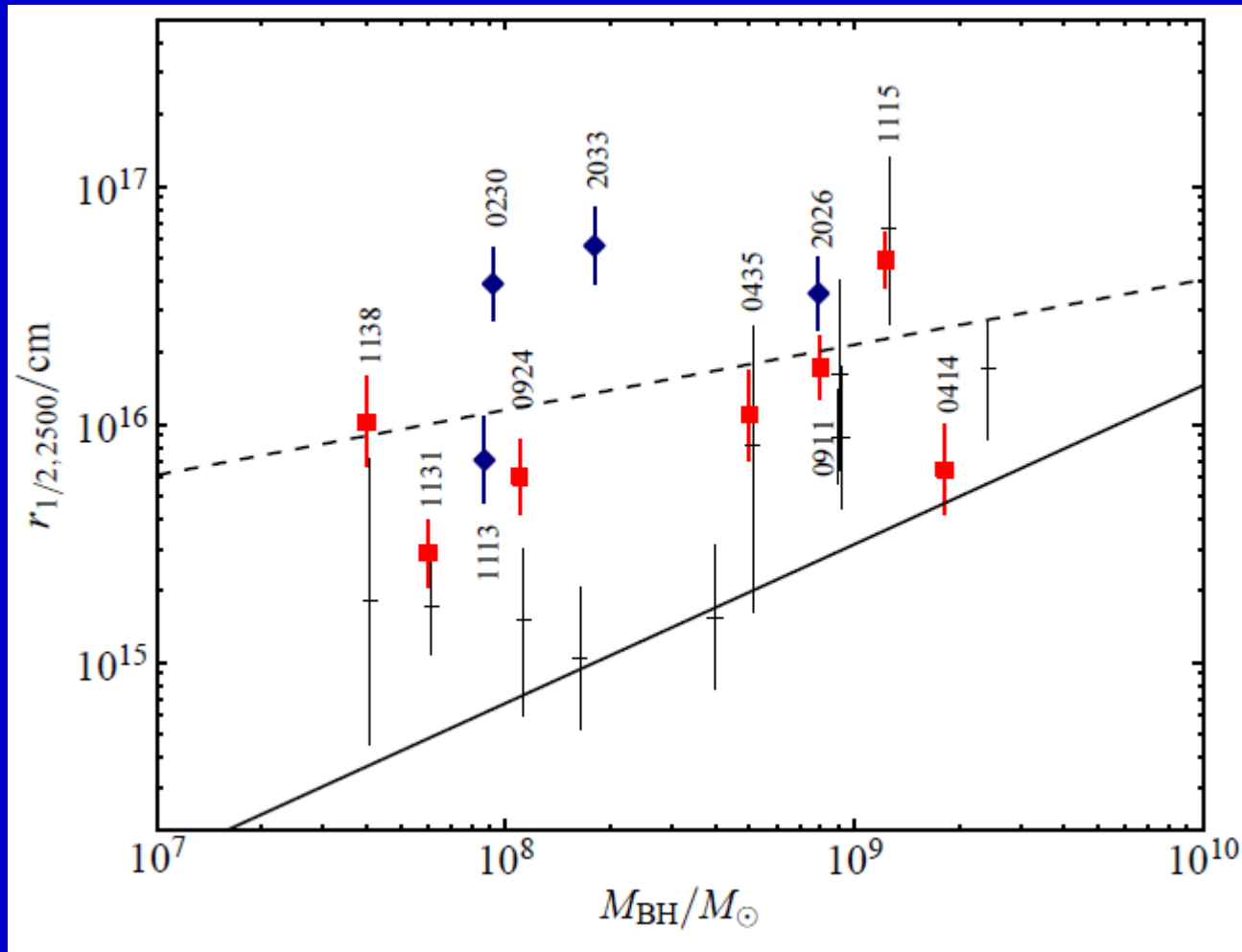
Using the data on microlensing at wavelengths 0.4-8 microns it was possible to derive the size of the disc in the quasar HE1104-1805 at different wavelengths.

Disc size – BH mass



Disc size can be determined from microlensing.

New data



IR and optics.

Chromatic microlensing:
blue light from
the inner regions
is more strongly
microlensed than
red light from farther out

Solid line is
the prediction
of the thin disk model.

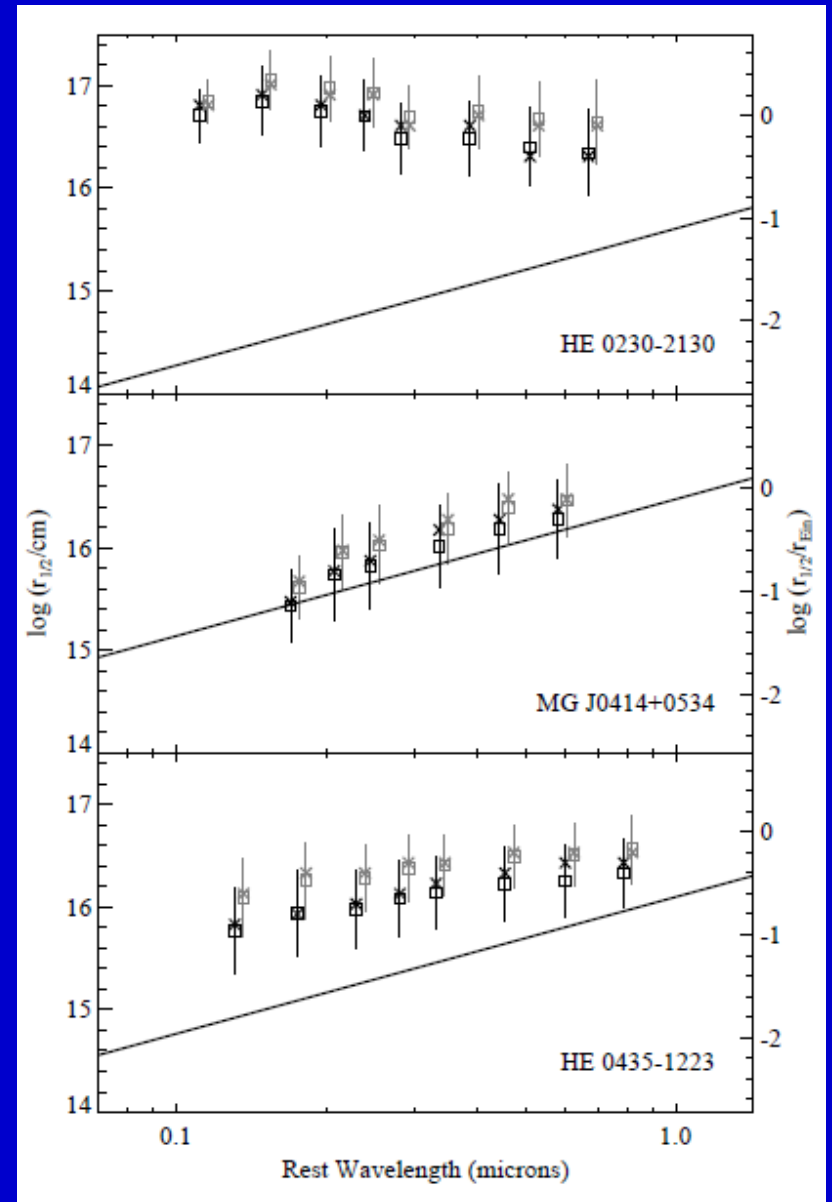
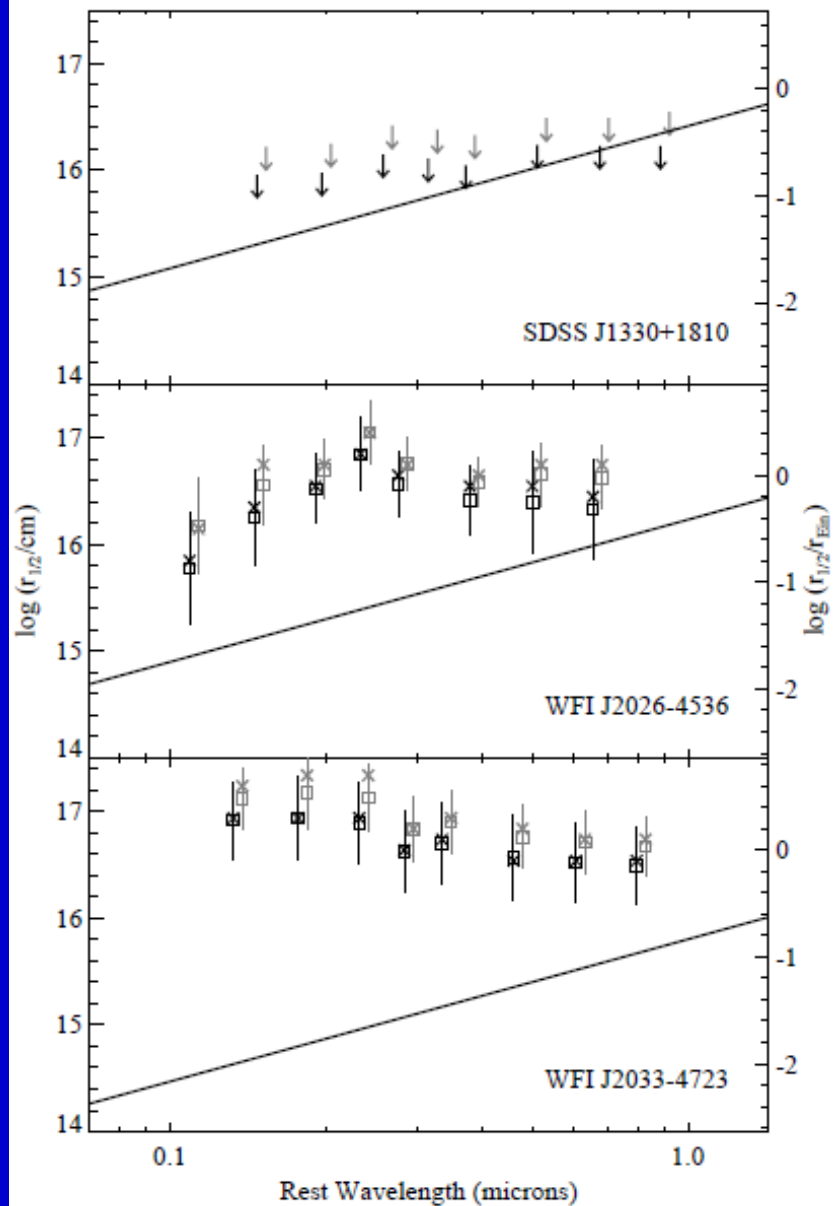
Standard disc properties

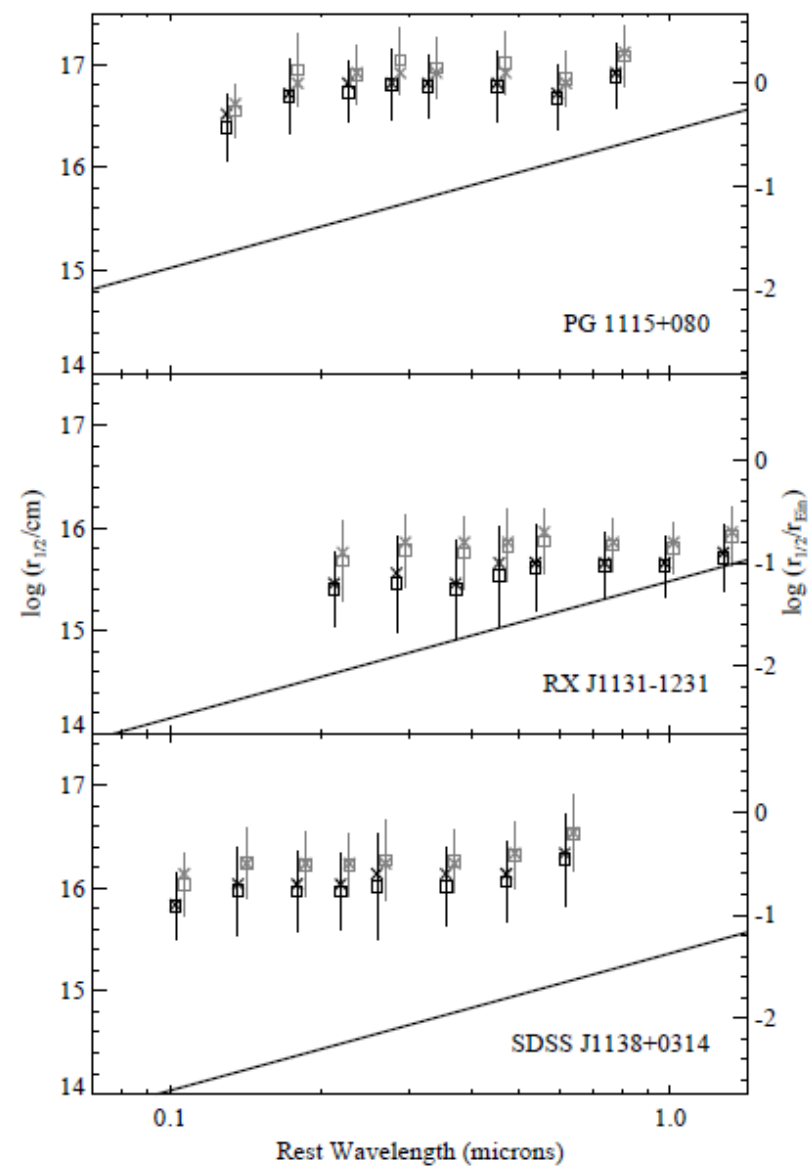
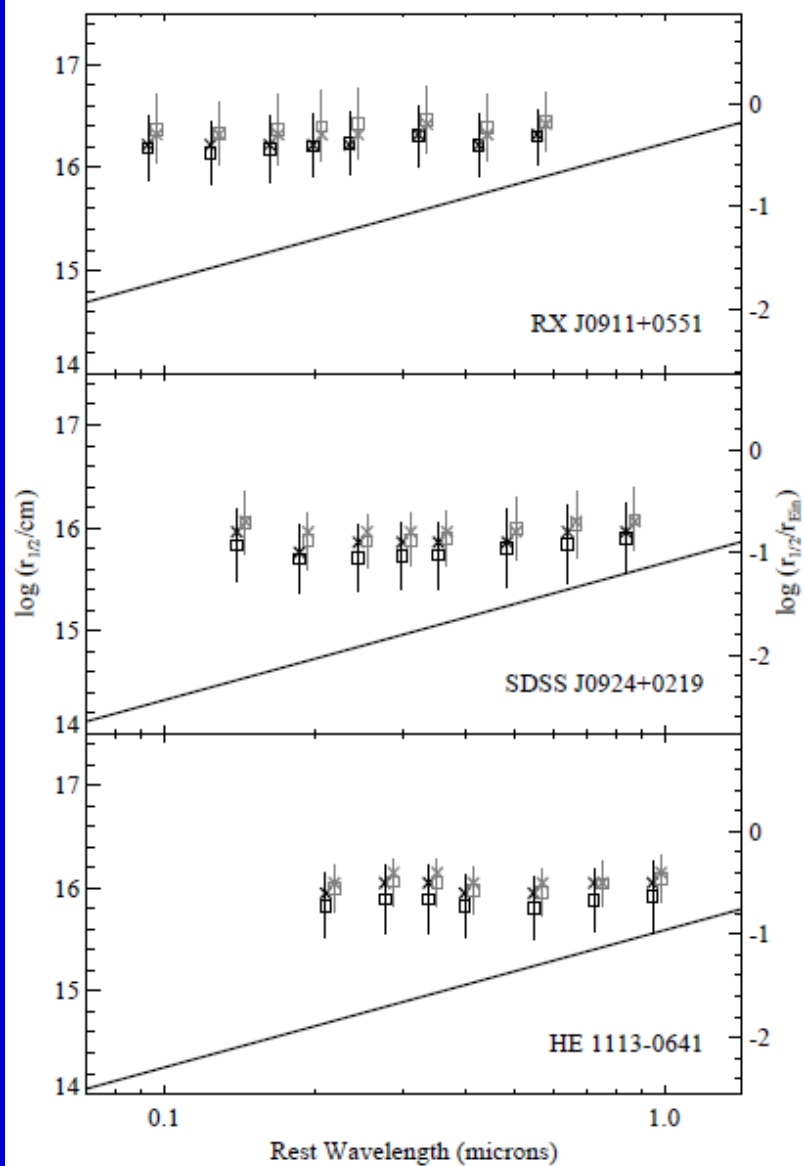
$$T_{\text{eff}}(r) = \left(\frac{3G^2 M_{\text{BH}}^2 m_p f_{\text{Edd}}}{2c\sigma_B \sigma_T \eta r^3} \right)^{1/4} g(r_{\text{in}}/r)^{1/4}$$

Standard disc model

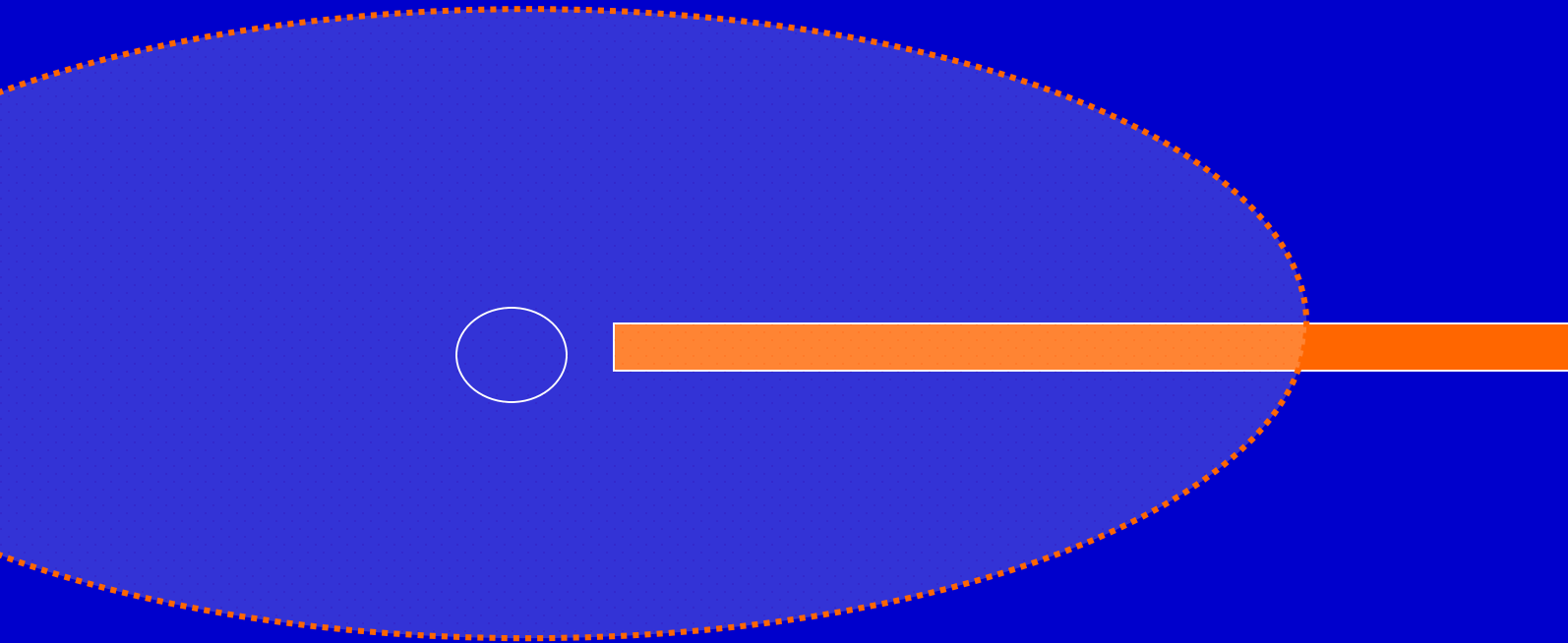
$$\begin{aligned} r_{1/2} &= 2.44 \left[\frac{45G^2 M_{\text{BH}}^2 m_p f_{\text{Edd}} \lambda^4}{4\pi^5 h_P c^3 \sigma_T \eta} \right]^{1/3} \sqrt{\cos i} \\ &= 1.68 \times 10^{16} \text{cm} \left(\frac{M_{\text{BH}}}{10^9 M_{\odot}} \right)^{2/3} \left(\frac{f_{\text{Edd}}}{\eta} \right)^{1/3} \left(\frac{\lambda}{\mu\text{m}} \right)^{4/3} \end{aligned}$$

$$r_{1/2} \sim \lambda^{4/3}$$





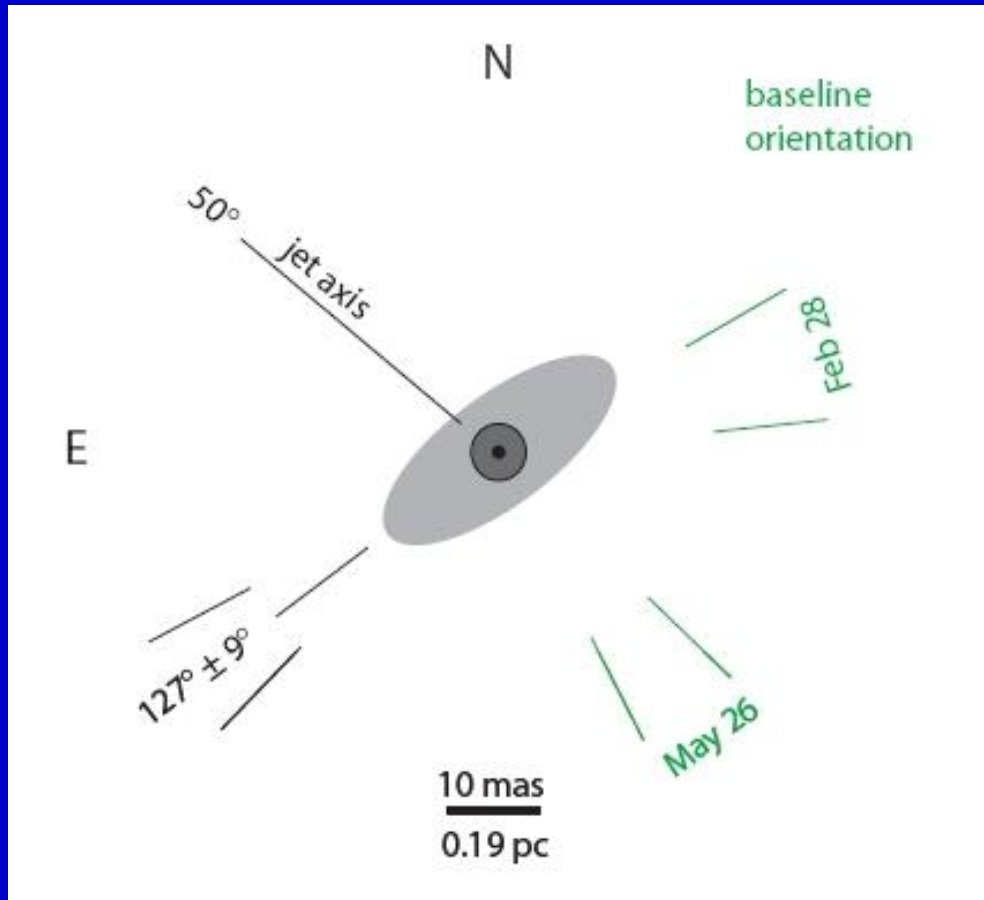
Super-Eddington discs



Super-Eddington accretion leads to formation of an optically-thick envelope scattering the radiation formed in the disc.

This makes the apparent disc size larger and practically independent of wavelength

Discs observed by VLTI



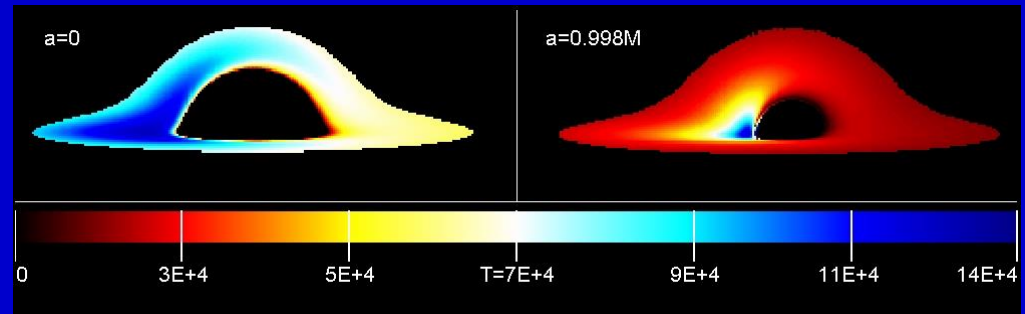
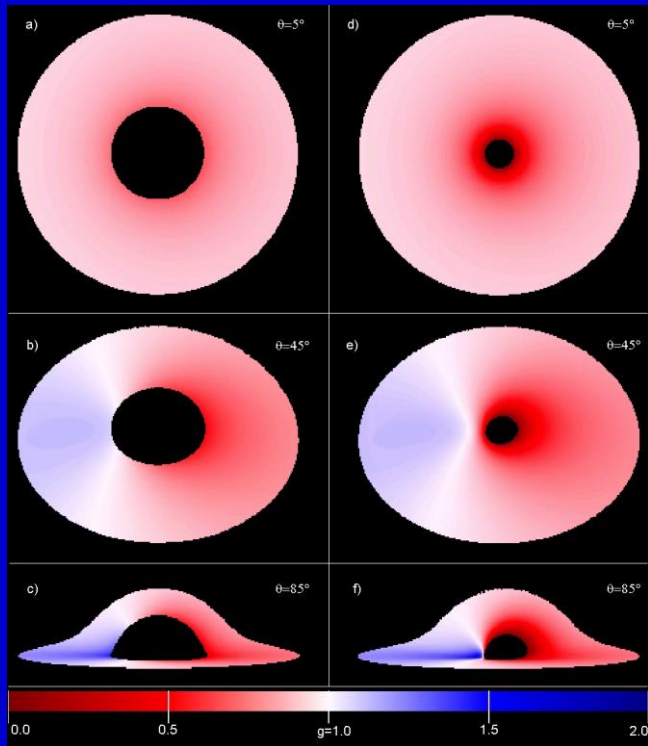
The structure of the disc in Cen A was studied in IR for scales $<1 \text{ pc}$.

The data is consistent with a geometrically thin disc with diameter 0.6 pc .

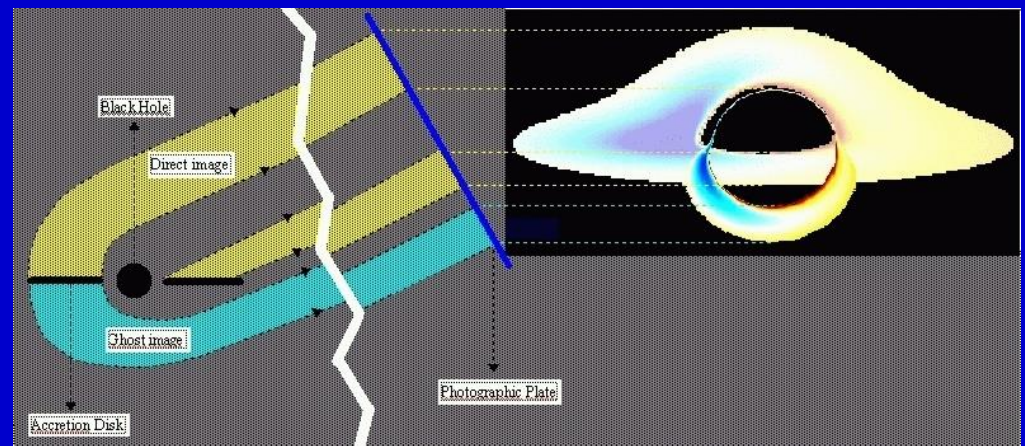
Observations on VLTI.

arXiv:0707.0177 K. Meisenheimer et al.
«Resolving the innermost parsec of Centaurus A at mid-infrared wavelengths»

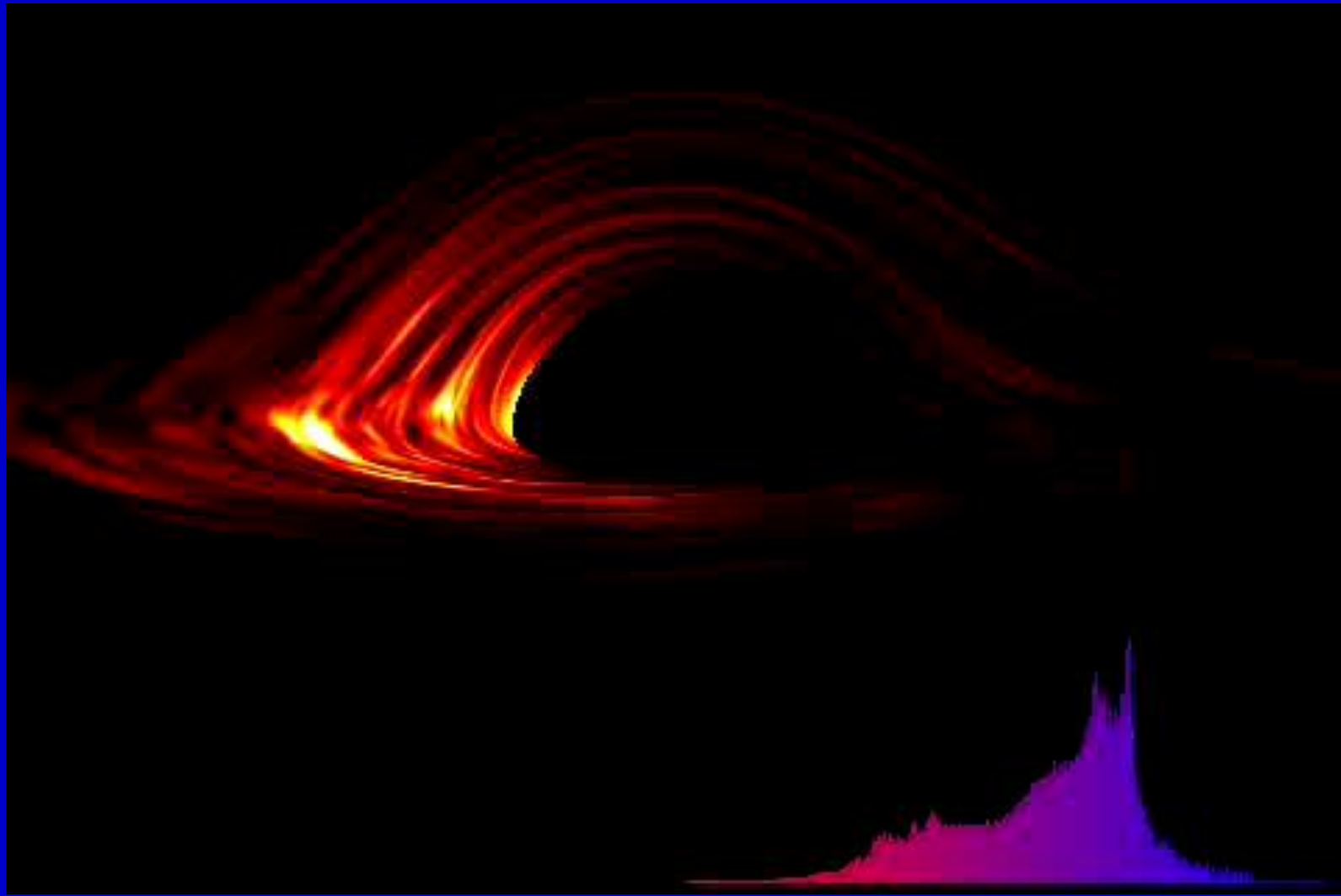
Discs around black holes: a look from aside



Disc temperature

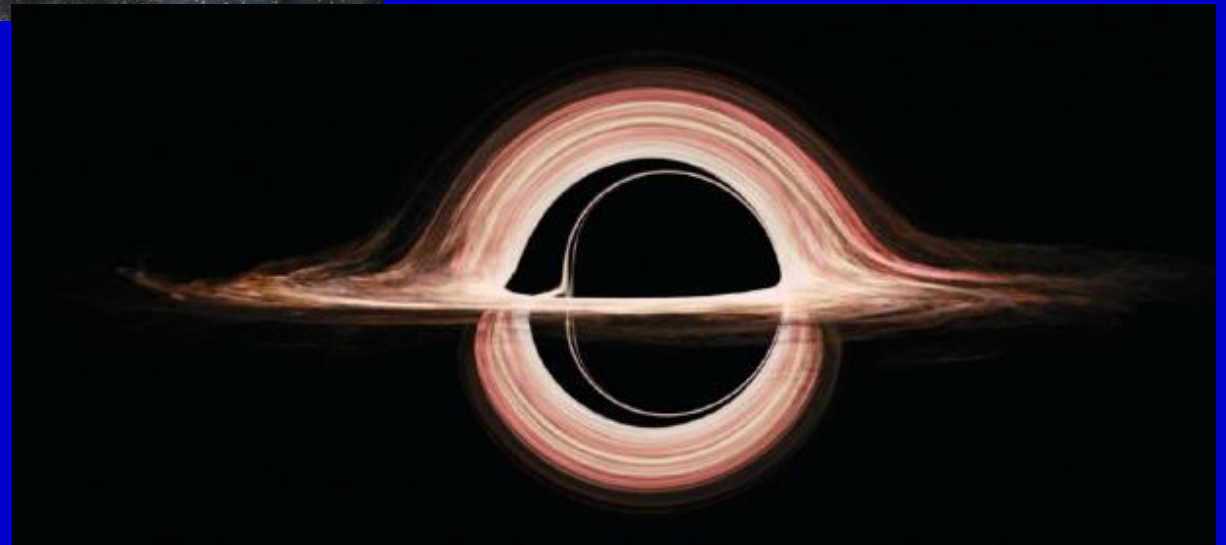
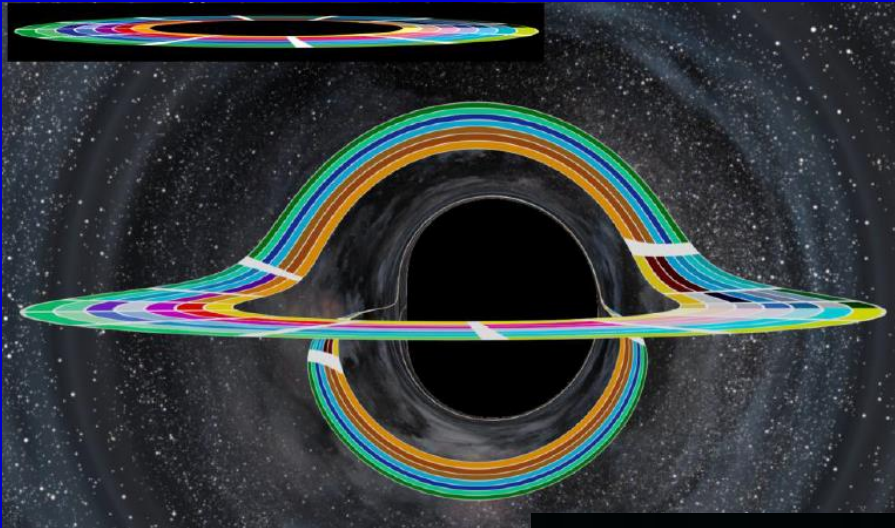


Discs observed from infinity.
Left: non-rotating BH,
Right: rotating.



from gr-qc/0506078

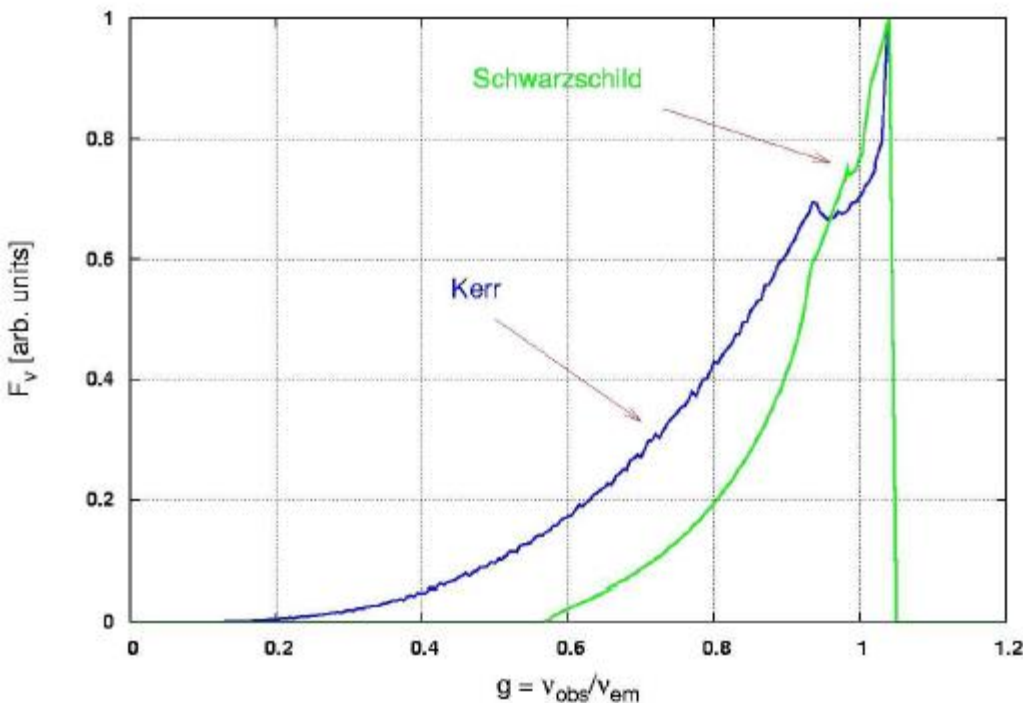
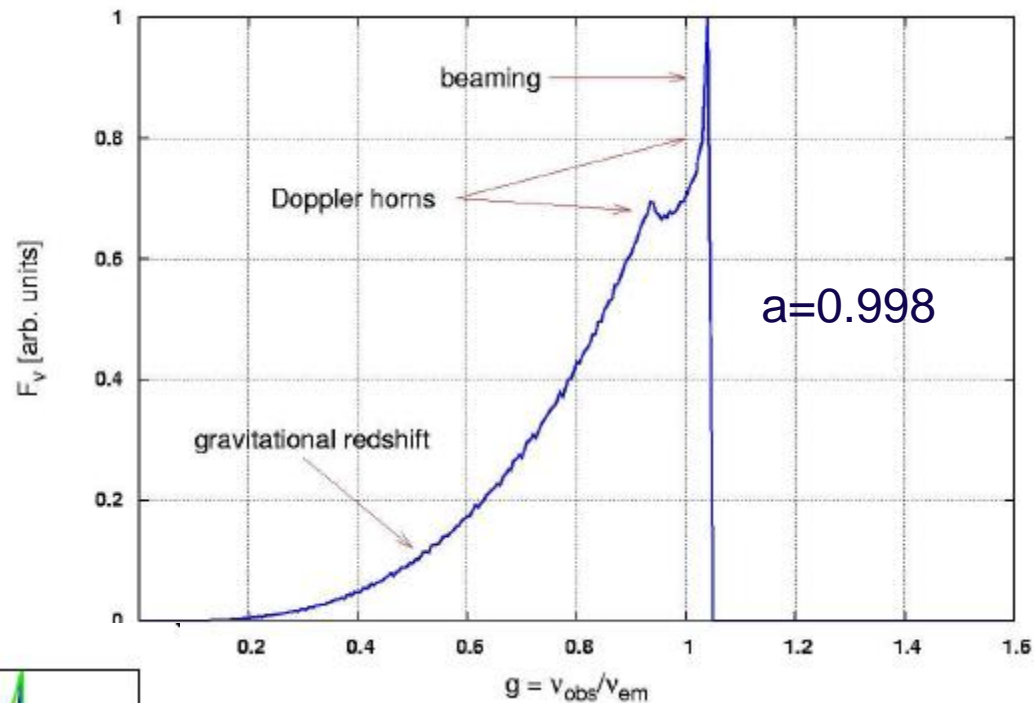
Discs from Interstellar movie



Different effects

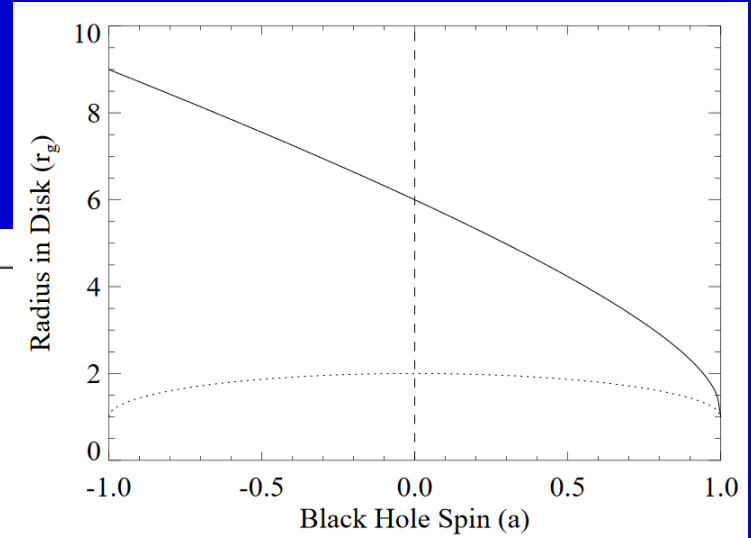
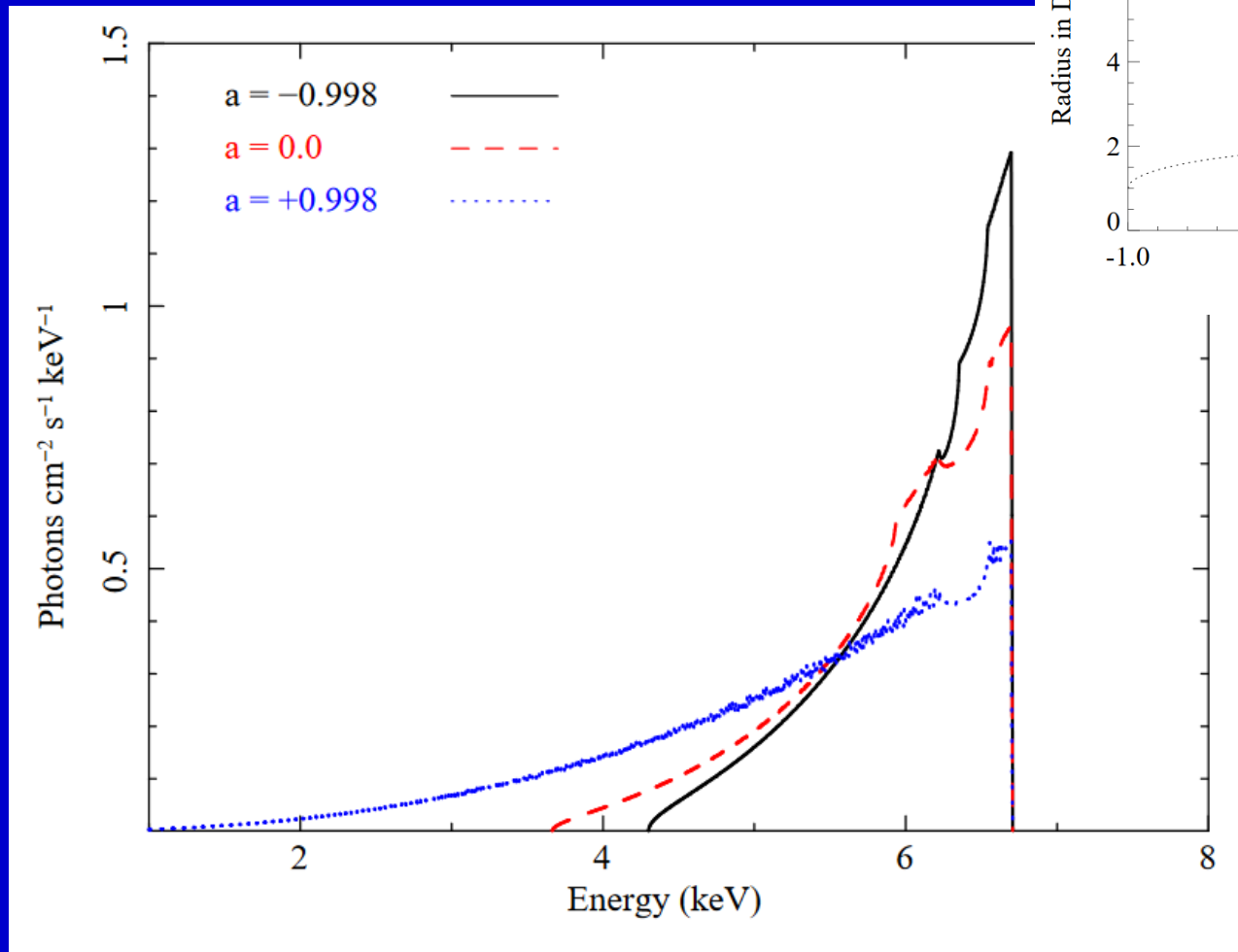
$$r_+ = \frac{GM}{c^2} + \left[\left(\frac{GM}{c^2} \right)^2 - \left(\frac{J}{Mc} \right)^2 \right]^{\frac{1}{2}}$$

For maximal rotation $r_{\text{ISCO}}=r_+$

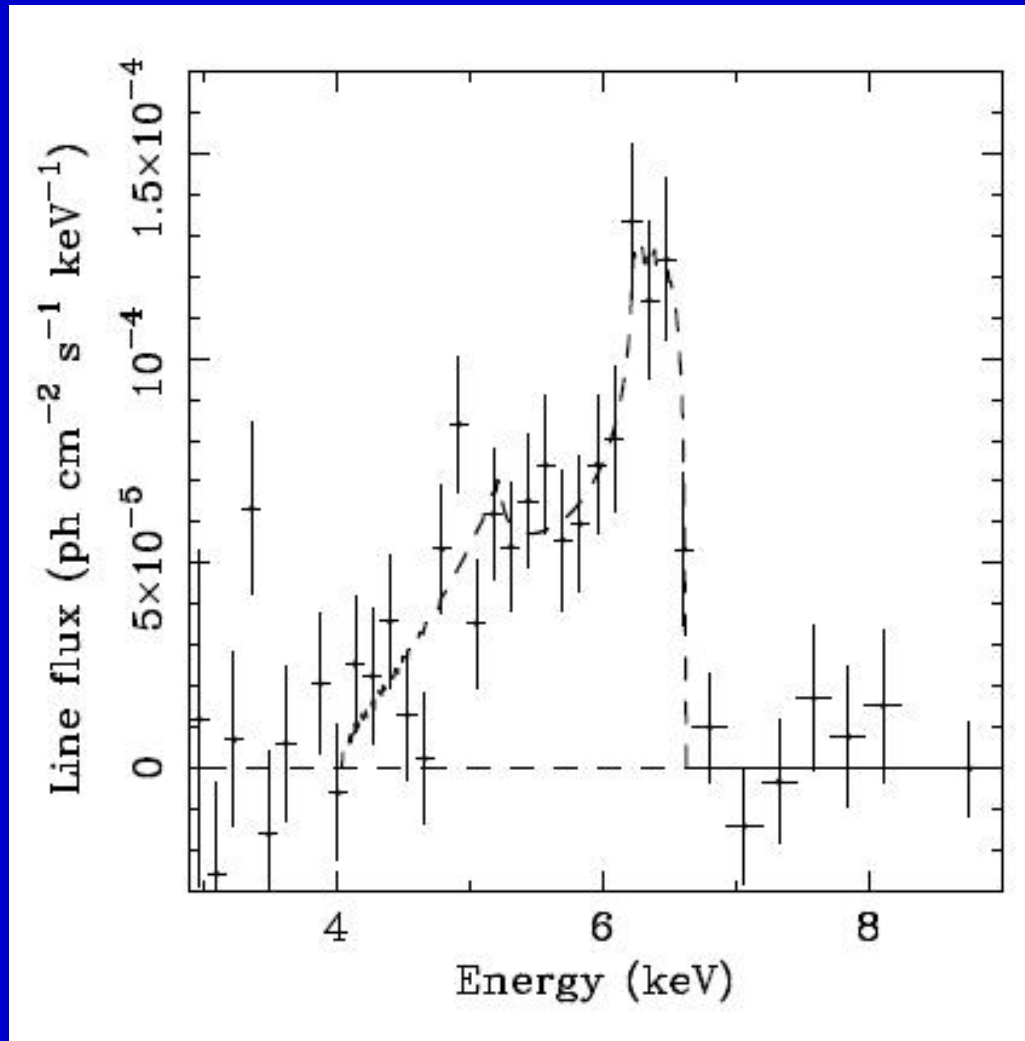


- Doppler effect
- Relativistic beaming
- GR light bending
- GR grav. redshift

Rotation direction



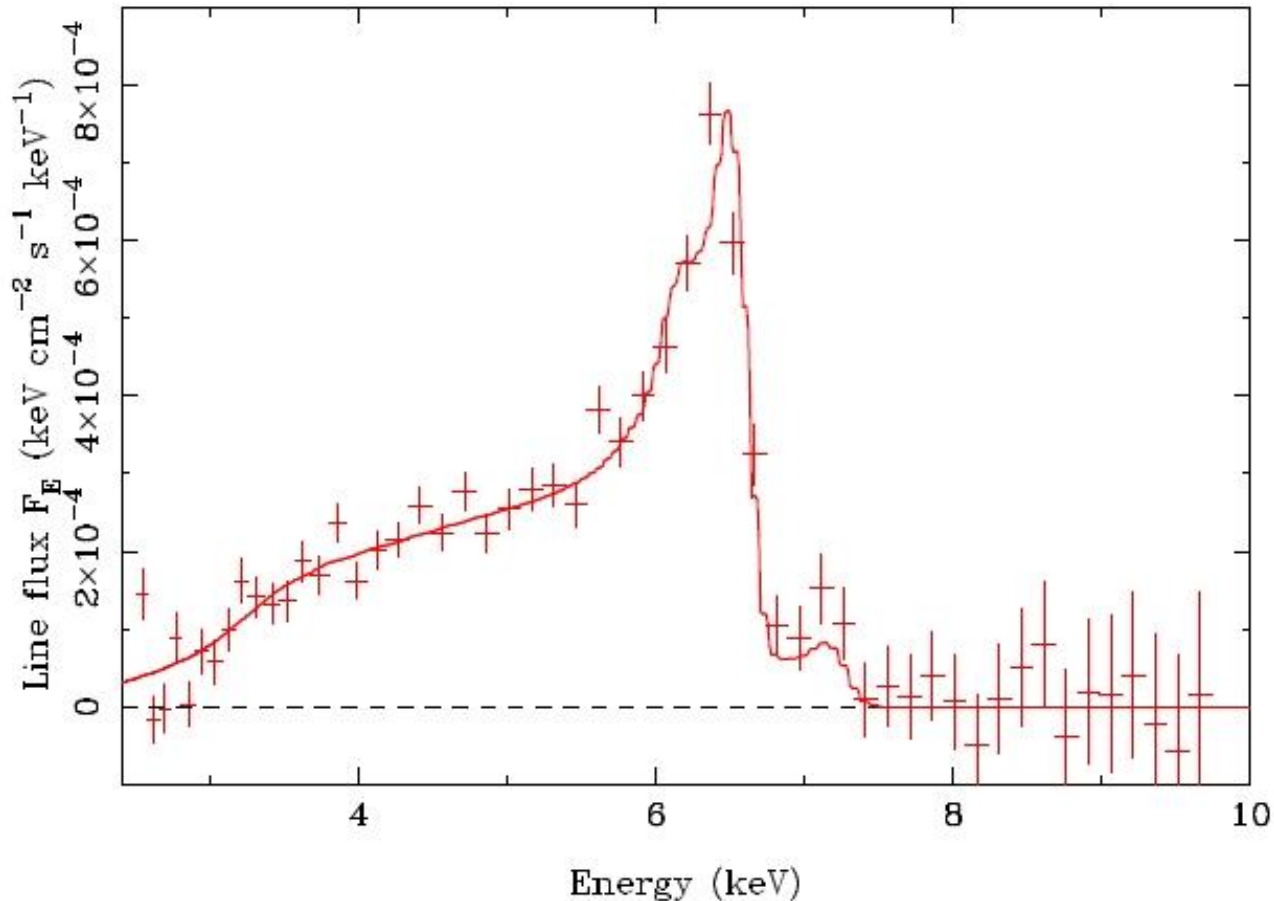
Fluorescent lines



The K α iron line observed by
ASCA (1994 r.).
Seyfert galaxy MCG-6-30-15

Dashed line: the model with
non-rotating BH,
disc inclination 30 degrees.

Lines and rotation of BHs



XMM-Newton data
(astro-ph/0206095)

The fact that the line extends to the red side below 4 keV is interpreted as the sign of rapid rotation (the disc extends inside $3R_g$).

see astro-ph/0212065

Suzaku spin measurements program

NGC 3783 $z = 0.00973$

A very complicated model.
 $a > 0.93$ (90% confidence)

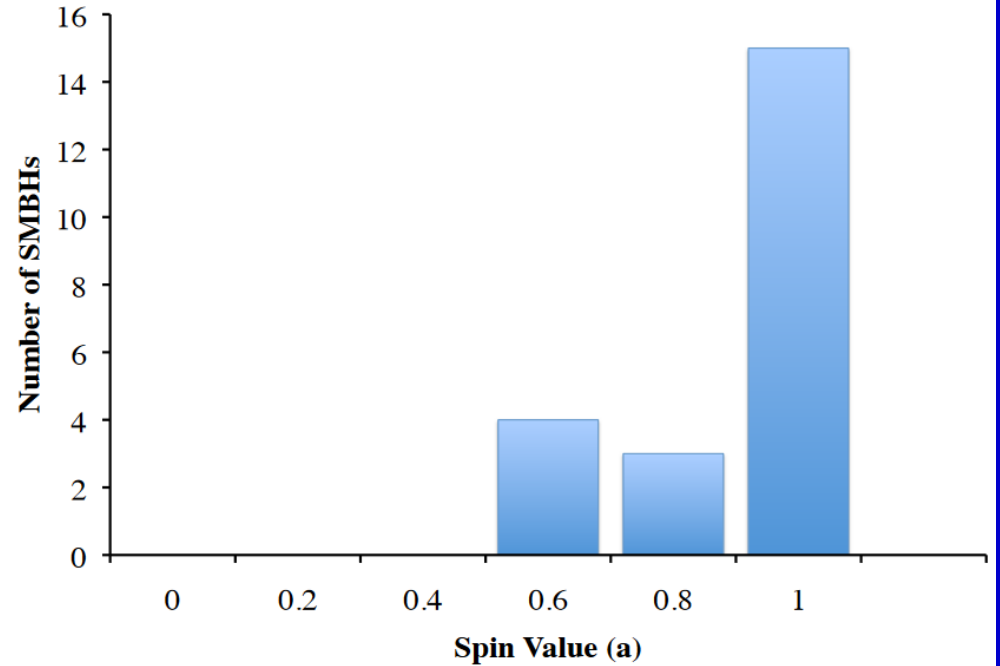
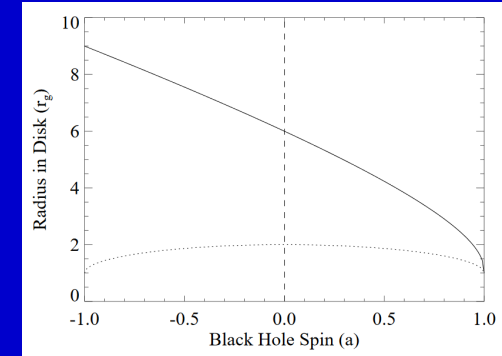
AGN	a
MCG-6-30-15 ^a	≥ 0.98
Fairall 9 ^b	$0.65^{+0.05}_{-0.05}$
SWIFT J2127.4+5654 ^c	$0.6^{+0.2}_{-0.2}$
1H0707-495 ^d	≥ 0.98
Mrk 79 ^e	$0.7^{+0.1}_{-0.1}$
Mrk 335 ^f	$0.70^{+0.12}_{-0.01}$
NGC 7469 ^f	$0.69^{+0.09}_{-0.09}$
NGC 3783 ^g	≥ 0.98

A little bit more data
in 1307.3246
and a big review in 1309.6334

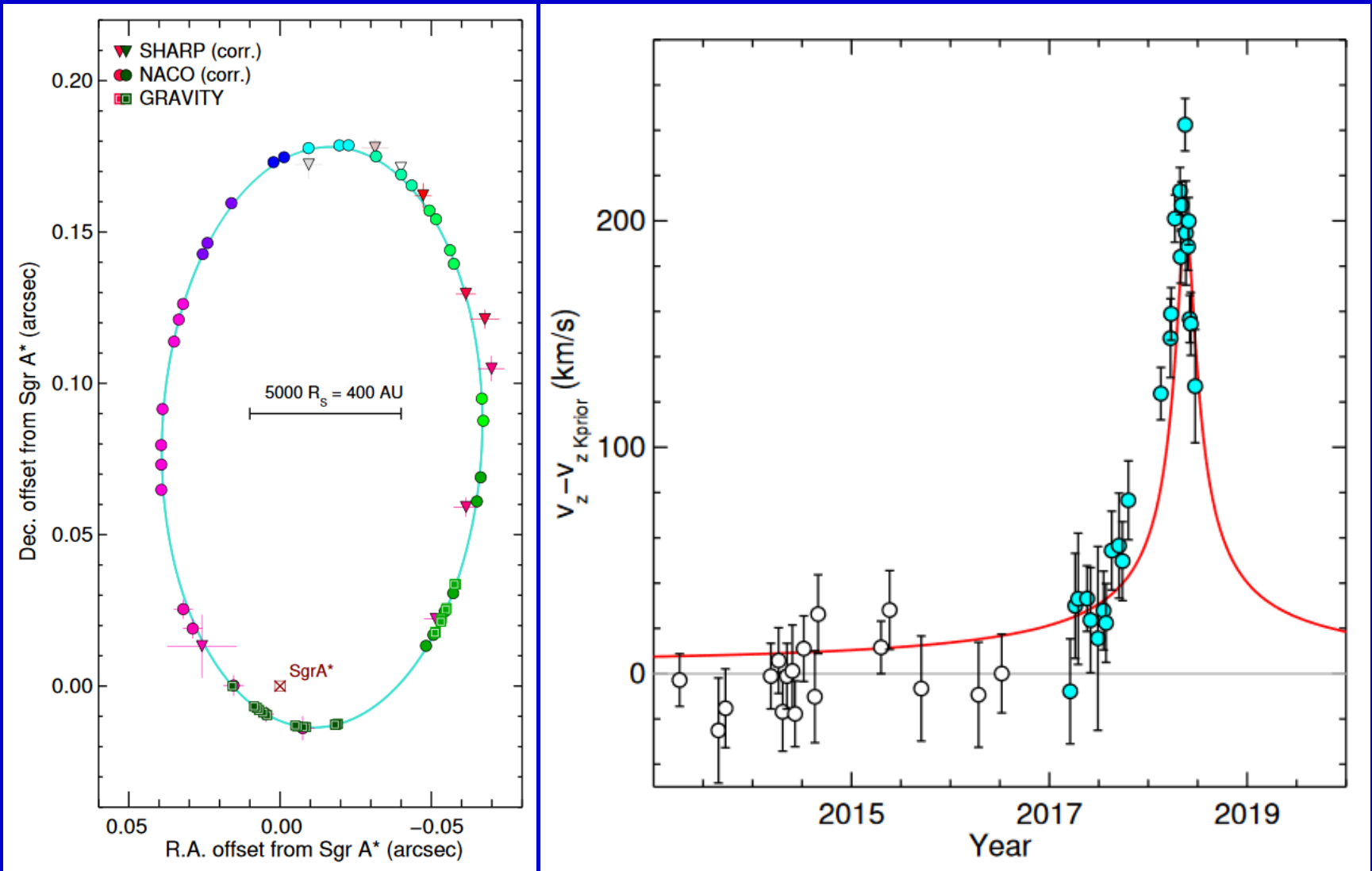


Relativistic reflection fitting of spectra

AGN	a	log M	$L_{\text{bol}}/L_{\text{Edd}}$	Host
MCG 6-30-15 ^a	$\geq +0.98$	$6.65^{+0.17}_{-0.17}$	$0.40^{+0.13}_{-0.13}$	E/S0
Fairall 9 ^b	$+0.52^{+0.19}_{-0.15}$	$8.41^{+0.11}_{-0.11}$	$0.05^{+0.01}_{-0.01}$	Sc
SWIFT J2127.4+5654 ^c	$+0.6^{+0.2}_{-0.2}$	$7.18^{+0.07}_{-0.07}$	$0.18^{+0.03}_{-0.03}$	—
1 H0707-495 ^d	$\geq +0.98$	$6.70^{+0.40}_{-0.40}$	$\sim 1.0_{-0.6}$	—
Mrk 79 ^e	$+0.7^{+0.1}_{-0.1}$	$7.72^{+0.14}_{-0.14}$	$0.05^{+0.01}_{-0.01}$	SBb
Mrk 335 ^f	$+0.70^{+0.12}_{-0.01}$	$7.15^{+0.13}_{-0.13}$	$0.25^{+0.07}_{-0.07}$	S0a
NGC 3783 ^g	$\geq +0.98$	$7.47^{+0.08}_{-0.08}$	$0.06^{+0.01}_{-0.01}$	SB(r)ab
Ark 120 ^h	$+0.94^{+0.1}_{-0.1}$	$8.18^{+0.05}_{-0.05}$	$0.04^{+0.01}_{-0.01}$	Sb/pec
3C 120 ⁱ	≥ 0.95	$7.74^{+0.20}_{-0.22}$	$0.31^{+0.20}_{-0.19}$	S0
1 H0419-577 ^j	$\geq +0.88$	$8.18^{+0.12}_{-0.12}$	$1.27^{+0.42}_{-0.42}$	—
Ark 564 ^j	$+0.96^{+0.01}_{-0.06}$	≤ 6.90	≥ 0.11	SB
Mrk 110 ^j	$\geq +0.99$	$7.40^{+0.09}_{-0.09}$	$0.16^{+0.04}_{-0.04}$	—
SWIFT J0501.9-3239 ^j	$\geq +0.96$	—	—	SB0/a(s) pec
Ton S180 ^j	$+0.91^{+0.02}_{-0.09}$	$7.30^{+0.60}_{-0.40}$	$2.15^{+3.21}_{-1.61}$	—
RBS 1124 ^j	$\geq +0.98$	8.26	0.15	—
Mrk 359 ^j	$+0.66^{+0.30}_{-0.54}$	6.04	0.25	pec
Mrk 841 ^j	$\geq +0.52$	7.90	0.44	E
IRAS 13224-3809 ^j	$\geq +0.995$	7.00	0.71	—
Mrk 1018 ^j	$+0.58^{+0.36}_{-0.74}$	8.15	0.01	S0
IRAS 00521-7054 ^l	$\geq +0.84$	—	—	—
NGC 4051 ^m	$\geq +0.99$	6.28	0.03	SAB(rs)bc
NGC 1365 ^k	$+0.97^{+0.01}_{-0.04}$	$6.60^{+1.40}_{-0.30}$	$0.06^{+0.06}_{-0.04}$	SB(s)b



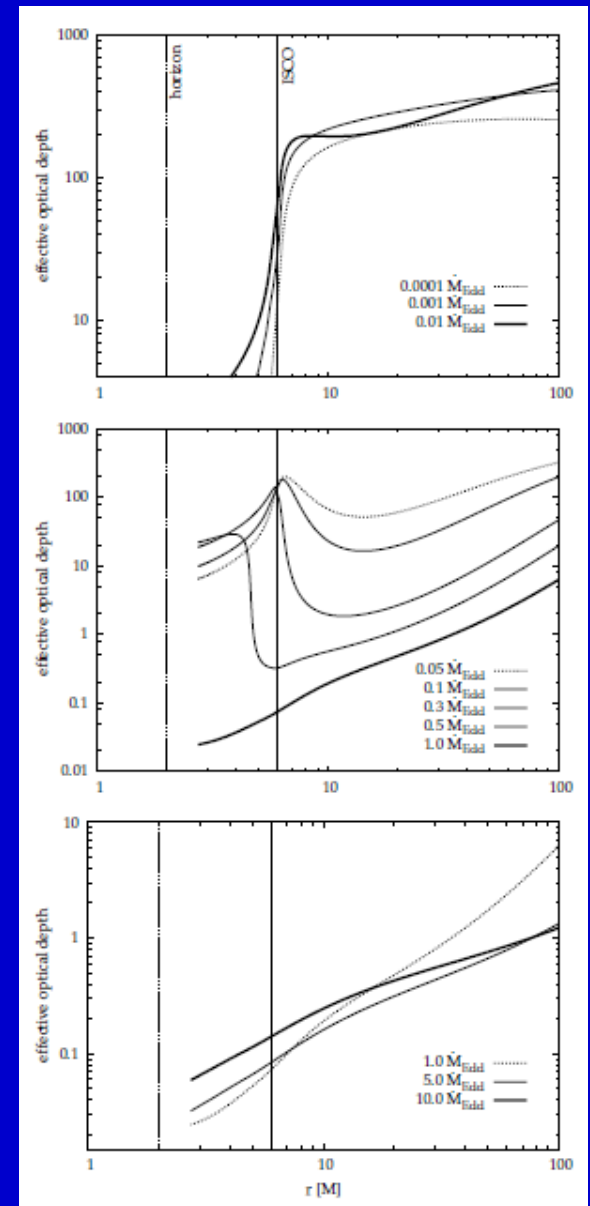
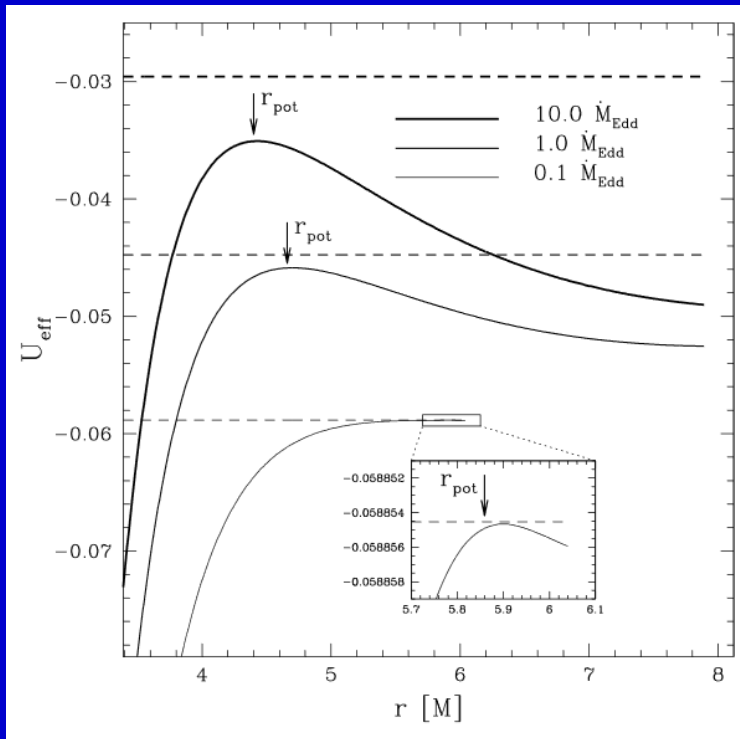
Gravitational redshift of the S2 star



The inner edge

The place where the fluorescent line is formed is not necessarily the standard ISCO.

Especially for large accretion rates the situation is complicated.



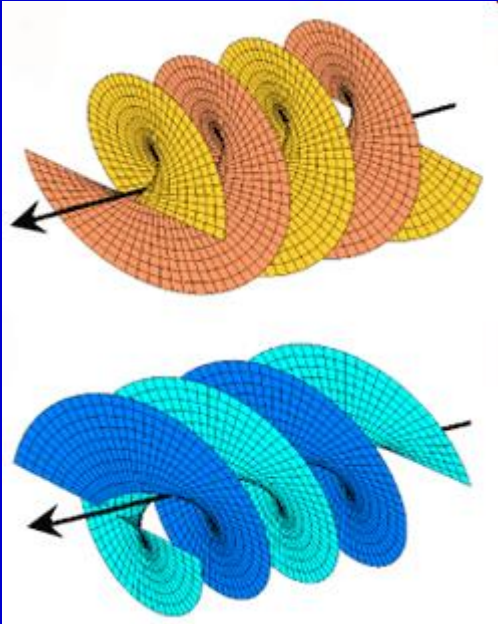
Measuring spins of stellar-mass BHs

Source	Spin a_*
GRS 1915+105	> 0.98
LMC X-1	$0.92^{+0.05}_{-0.07}$
M33 X-7	0.84 ± 0.05
4U 1543-47	0.80 ± 0.05
GRO J1655-40	0.70 ± 0.05
XTE J1550-564	$0.34^{+0.20}_{-0.28}$
LMC X-3	$< 0.3^b$
A0620-00	0.12 ± 0.18

Different methods used
1101.0811

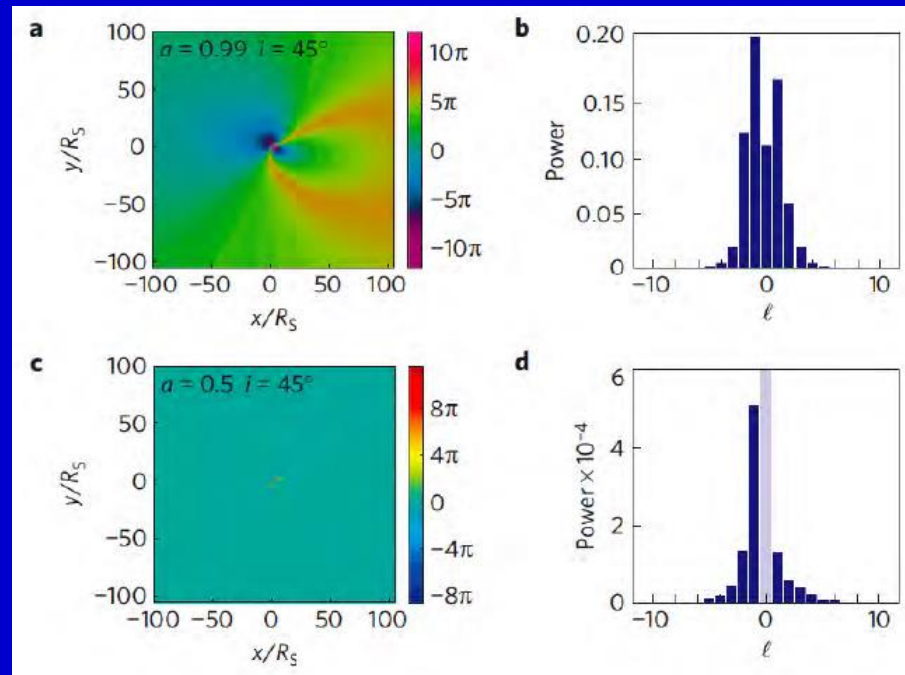
See a review on BH spin
(both XRB and AGN) in
1507.06153

Twisted light



This effect can be used to learn about spin of accreting BHs.

If the source of the gravitational field also rotates, it drags space-time with it. Because of the rotation of the central mass, each photon of a light beam propagating along a null geodesic will experience a well-defined phase variation.



1104.3099

See <http://www.physics.gla.ac.uk/Optics/play/photonOAM/>
and astro-ph/0307430 about orbital angular momentum of photons